Atmospheric Environment 299 (2023) 119650

Contents lists available at ScienceDirect

Atmospheric Environment

journal homepage: www.elsevier.com/locate/atmosenv

Chemical composition and potential sources of $PM_{2.5}$ in Hanoi

Ulla Makkonen [a,*], Mika Vestenius [a], L.N. Huy [b], N.T.N. Anh [c], P.T.V. Linh [c], P.T. Thuy [c], H.T.M. Phuong [c], Huyen Nguyen [d], L.T. Thuy [d], Minna Aurela [a], Heidi Hellén [a], Katja Loven [a], Rostislav Kouznetsov [a], Katriina Kyllönen [a], Kimmo Teinilä [a], N.T. Kim Oanh [b]

[a] Finnish Meteorological Institute, Erik Palmenin Aukio 1, 00560, Helsinki, Finland
[b] Environmental Engineering and Management, Asian Institute of Technology, Klongluang, Pathumthani, Thailand
[c] Northern Centre for Environmental Monitoring (NCEM), Viet Nam
[d] Environmental Protection Agency Hanoi (Hanoi EPA), Viet Nam

HIGHLIGHTS

- Highest daily concentrations occurred during winter with stagnant meteorological conditions.
- Half of resolved $PM_{2.5}$ mass was organic matter of which about 40% attributable to biomass burning.
- One third of $PM_{2.5}$ mass was secondary inorganic aerosol dominated by sulphates.
- With the PMF analysis following source factors were found LRT and local SIA, traffic, biomass burning, industry and dust.
- During the COVID-19 lockdown period concentration of elemental carbon was halved at the traffic site.

GRAPHICAL ABSTRACT

Chemical composition of $PM_{2.5}$ resolved mass.

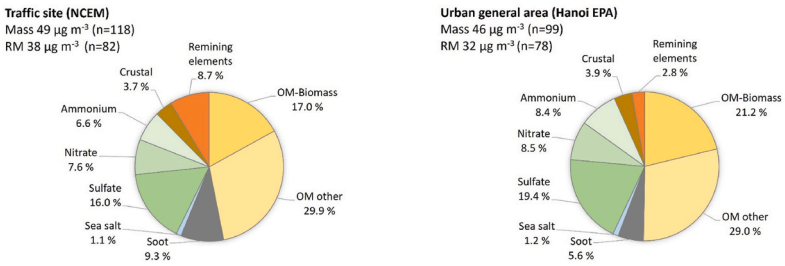

ARTICLE INFO

Keywords:
$PM_{2.5}$
Hanoi air quality
Source apportionment
PMF
Levoglucosan
Chemical composition
COVID-19 lockdown
Air pollution
Biomass burning

ABSTRACT

The chemical composition of $PM_{2.5}$ was monitored simultaneously at two sites, one in a general area of the city center and one at a roadside, in Hanoi, Vietnam, during August 2019–July 2020 using 220 daily (24 h) filter samples. PM mass, water soluble ions, trace elements, organic and elemental carbon and sugar anhydrides were measured. The annual average $PM_{2.5}$ concentrations, 49 and 46 μg m^{-3} at the traffic and the general urban site, respectively, exceeded the national (25 μg m^{-3}) and 2021 WHO limit values (5 μg m^{-3}). Daily $PM_{2.5}$ concentrations were the highest in winter when stagnant meteorological conditions prevailed. On average, half of the resolved mass was organic matter, of which about 40% was attributable to biomass burning, most likely rice straw field burning and domestic fuel combustion. One third of $PM_{2.5}$ was secondary inorganic aerosol which was dominated by sulphate hence indicating a high contribution of stationary sources like coal combustion. The elemental carbon level was higher at the traffic site, except in April 2020 during the COVID-19 restrictions. Zinc was the most common trace element with high daily variations and large differences between the sites, and it often peaked with Cd, Cl^- and Pb indicating contribution of industrial sources and/or coal combustion. The highest zinc concentrations appeared on a few days and likely originated from open burning of municipal solid waste. It appeared that scattered open waste and biomass burning, as well as coal combustion, are important

* Corresponding author.
E-mail address: ulla.makkonen@fmi.fi (U. Makkonen).

https://doi.org/10.1016/j.atmosenv.2023.119650
Received 23 June 2022; Received in revised form 16 December 2022; Accepted 25 January 2023
Available online 14 February 2023

sources causing spikes of $PM_{2.5}$ pollution in Hanoi above the general levels caused by routine industrial and traffic sources, especially during stagnant winter days. Source contributions were further studied with positive matrix factorization producing six source factors: traffic (12%), local secondary inorganic aerosol (SIA, 18%), biomass burning (19%), industry (9%), long-range transported SIA (25%) and dust (17%).

1. Introduction

Air pollution, especially with high levels of fine particles ($PM_{2.5}$), is a severe concern globally but more so for densely populated Asian cities (Hopke et al., 2008; Kim Oanh et al., 2006). Hanoi, the capital of Vietnam, with its fast-growing population and economy is increasingly facing challenges of maintaining and improving air quality. The available monitoring data has shown that the annual average concentrations of $PM_{2.5}$ have exceeded the national ambient air quality standard (NAAQS) of Vietnam (25 μg m^{-3}, (QCVN 05, 2013) and by far exceeded the recently updated World Health Organization (WHO) air quality guideline (5 μg m^{-3}, WHO, 2021a). Exposure to these fine particles, which penetrate deep in the lungs, causes respiratory and cardiovascular diseases and premature deaths (HEI, 2020; Nhung et al., 2018; Luong et al., 2020; Lu et al., 2019; Phung et al., 2016; Xing et al., 2016; Jalava et al., 2007). The WHO (2021b) has estimated that around 60 000 deaths each year are related to air pollution in Vietnam. In Hanoi, high $PM_{2.5}$ concentrations are observed, especially in winter when drier weather is prevalent under the influence of the Northeast Monsoon as compared to summertime. Stagnant meteorological conditions limited wet removal and more biomass open burning occurring around the city during winters are some of the most important reasons for the high build-up of PM pollution in Hanoi (Kim Oanh, 2021; Hai and Kim Oanh, 2013). Regionally, the potential long-range transportation from Northern Vietnam and China associated with the Northeast Monsoon (Ly et al., 2021; Cohen et al., 2010a, 2010b) also contribute to the high pollution levels during winter. Increased concentrations of air pollutants during winter are found to increase the number of hospital visits due to acute respiratory and cardiovascular diseases (Trinh et al., 2019).

In addition to the mass concentrations, the chemical composition of particles influences their harmfulness to people, e.g., a strong and consistent correlation with mortality has been found for combustion species such as elemental carbon (EC) and potassium (Achilleos et al., 2017). These fine particles from combustion sources also contain carcinogenic organic compounds such as polycyclic aromatic hydrocarbons (PAHs) and other toxic elements (e.g., arsenic, cadmium, lead) that increase health risks (Holme et al., 2019). In addition to health effects, particulate pollution leads to haze formation and decreases visibility (Ngoc et al., 2021). Finally, particulate matter (PM) affects the climate, especially the black carbon (BC) particles emitted from incomplete combustion can increase global warming (Ramanathan and Carmichael, 2008).

In Northern Vietnam, there is a wide range of industrial sources such as large industrial plants, mines, smelters, and small industrial workshops scattered in populated craft villages, emitting particles containing various trace elements. Coal-fired power plants, e.g., the Pha Lai thermal coal-fired power plant complex in Hai Duong Province, which is about 65 km north-east of Hanoi, are the major power generation sources in the country (Huy and Kim Oanh, 2017; Roy et al., 2021). Dust from cement industrial plants scattered in Northern Vietnam and the intensive construction activities in the fast-growing areas of Hanoi, as well as road dust also contribute to PM pollution. Agricultural burning, e.g., the common practice of rice straw burning, is an important emission source in rural and suburban areas (Le et al., 2020; Kim Oanh et al., 2011; Kim Oanh, 2021). Backyard solid waste open burning is still a common practice outside the city center where solid waste collection coverage is still limited. In remote rural areas, agricultural residues, fuel wood, and derived coal fuel are still popularly used for cooking despite the increasing use of gas and electricity (Huy et al., 2021). The intensive use of diesel vehicles, both on-road and off-road, is an important source of PM including BC, and precursors gases (Kim Oanh et al., 2010), NOx, SOx, and hydrocarbons which form secondary particles in the atmosphere. Furthermore, the large fleets of gasoline-powered motorcycles and scooters increase the resuspension of road dust especially during the rush hours hence elevating the PM levels in Hanoi (Kim Oanh, 2021), and the large amounts of precursor gases released from the vehicle exhausts also contribute to the formation of secondary particles (Ly et al., 2020; Phuc and Oanh, 2018, 2021). In addition to the local sources, long-range transportation from the north and north-east contribute significantly to $PM_{2.5}$ levels (Cohen et al., 2010b; Ly et al., 2021; Kim Oanh, 2021).

In Hanoi, continuous $PM_{2.5}$ monitoring has been carried out by the local authorities: Northern Center for Environmental Monitoring (NCEM) of the Vietnam Environment Administration (VEA) from the Ministry of Natural Resources and Environment (MONRE; http://cem.gov.vn/) and the Hanoi Environmental Protection Agency (EPA) from the Hanoi Department of Natural Resources and Environment (DONRE; http://moitruongthudo.vn). The air quality data has been available for the public. However, there are no routine measurements of the chemical composition of $PM_{2.5}$, and there is still limited updated information of source apportionment for $PM_{2.5}$ in the city.

In this paper, we present and analyze a one-year dataset of the $PM_{2.5}$ chemical composition measured in two locations in Hanoi city during 2019–2020 to reveal the seasonal variations and potential contributing sources. The data were also studied with positive matrix factorization (PMF), which is a widely used source apportionment tool (Hopke et al., 2020). Selected days with high $PM_{2.5}$ concentrations were studied in detail with trajectories and fire hotspot maps.

2. Methodology

2.1. Description of the study area and measurement sites

Hanoi capital city is located within the Hanoi Metropolitan Region (HMR) which had a population of over 8.2 million and an average population density of 2455 people/km^2 as of 2019 (GSO, 2020). HMR is in the Red River Delta, about 100 km from the coast of Gulf of Tonkin. Weather in Hanoi is influenced by the tropical monsoon climate, typical for Northern Vietnam, with two main seasons, i.e., winter (November to March) and summer (May to September), and two transitional periods in between: spring (April) and autumn (October) (Ngu and Hieu, 2004). In winter, high-pressure ridges are frequently observed extending from central China to Northern Vietnam that bring in cold weather spells with associated low mixing heights and calm wind, typically for areas under the influence of stable high-pressure systems. When prevalent, these conditions enhance the accumulation of ambient air pollution to considerably high levels during winters in the city (Hai and Kim Oanh, 2013; Hien et al., 2011; Kim Oanh et al., 2006).

Road traffic, open burning (rice straw), industrial activities and construction activities release a large amount of PM2.5 into the atmosphere together with the gaseous precursors of NOx, SOx and volatile hydrocarbons for secondary PM formation. The traffic fleet is dominated by motorcycles: there are more than 5.6 million registered motorcycles compared to 0.6 million cars in Hanoi (GSO, 2020), and serious congestion problems appear on some roads during rush hours. Vehicle movement on dusty roads in the city resuspend coarse and fine PM which are confirmed by monitoring data (Kim Oanh, 2021). Hanoi is located downwind of several provinces in Northern Vietnam including

those having intensive industrial activities, such as Thai Nguyen, Quang Ninh, Bac Ninh, and Hung Yen, hence when the Northeast Monsoon is prevalent in the dry winter season, there is a high potential of regional transport on the top of the transboundary transport of the pollution.

Two measurement sites in Hanoi city were selected in this study to represent the urban general area of the city center (UGA site) and roadside air quality (traffic site). The measurement sites were located about 10 km apart. The measurement site on the roof of Hanoi EPA office building (21° 0′ 53.9″ N, 105° 48′ 1.9″ E; 15 m above ground) in the west side of the city center was selected as the UGA site. It is surrounded by a park on two sides and 4–6 floor buildings on the other two sides. The CT20 ring road is less than 2 km west from the UGA site. The NCEM measurement station, (21° 2′ 56.3″ N, 105° 52′ 56.3″ E; 3 m above ground) represented a traffic site (Fig. S1). The NCEM station is located within 5 m from the 3-lane road 556 Nguyen Van Cu, right at the gateway to the inner city. The street is of a semi-street canyon configuration. The site is located next to a 6-floor office building of NCEM and surrounded on the same side with similar 4–6 floor buildings of offices and apartments. The $PM_{2.5}$ samplers were located on the roof of the NCEM measurement container.

2.2. Measurement methods

During the one-year measurement period (August 6, 2019–August 6, 2020), about 220 filter samples were collected for gravimetric analysis, i.e., in total 120 at the NCEM traffic station and 100 at the Hanoi EPA UGA station. The target was to collect samples at both sites on the same days, but unfortunately this was not completely fulfilled, and during COVID-19 there were challenges to continued sampling. Sampling was done according to the standard EN 12341:2014. At both sites, two parallel low volume samplers (Leckel LVS/LVS6-RV) with EU type $PM_{2.5}$ sampling heads and a flowrate of 2.3 m^3/h were installed to collect 24 h samples from midnight to midnight in intervals of 2–3 days. The air flow, temperature and pressure measurements of the samplers had been calibrated by the manufacturer. The validity of the air flow was verified using a SI-traceable TSI 4043 flow meter calibrated by the Finnish Meteorological Institute (FMI) calibration laboratory before the measurement campaign. Two samples were discarded because of malfunction of the sampler. Initially quartz fiber filters (Tissuquartz 2500AT-UP, 47 mm, Pall Life Sciences, no. 7202) were used in both instruments which were subsequently used for both gravimetric and chemical analysis. However, in October 2019, it was noticed that the quartz filter was not suitable for the weighing process in the humid conditions of Hanoi, and hence the filter material for the gravimetric analysis was changed to a glass microfiber filter (Grade MG227/1/60 47 mm, Ahlstrom Munksjo, no. 443 005) which proved to be satisfactory for weighing. The gravimetric analysis was conducted at NCEM using a Sartorius ME-5 microbalance (resolution μg, repeatability ± 1 μg, precision 5.8 μg). Filter conditioning for pre- and post-weighing was done following the procedure specified in U.S. EPA (2013).

A total of 160 quartz filter samples, 82 from the NCEM traffic site and 78 from the Hanoi EPA UGA site and ten trip blank samples from each station, were analyzed for the chemical composition of water-soluble ions, trace elements, EC, and organic carbon (OC), and monosaccharide anhydrides including levoglucosan at the FMI. The quartz filters selected for the chemical analysis were punched to get four 1 cm^2 filter pieces for analysis.

Water-soluble inorganic ions (NO_3^-, SO_4^{2-}, Cl^-, NH_4^+, Na^+, K^+, Mg^{2+}, and Ca^{2+}) were analyzed according to the standard EN 16913:2017b with two ion chromatographs (Waters Corporation). Trace elements (Al, As, Cd, Co, Cr, Cu, Fe, Mn, Ni, Pb, V, and Zn) were analyzed with an inductively coupled plasma mass spectrometer (ICP-MS, Thermo iCAP Q) according to the standard EN 14902:2005, see Kyllönen et al. (2020) for details. OC and EC were analyzed using thermal-optical techniques based on the evolution of carbon species at different temperatures in an oxidizing environment using the EC-OC Lab Instrument (Model 5, Sunset Laboratory Inc). The method and temperature protocol (EUSAAR2, Cavalli et al., 2010) were based on the standard EN 16909:2017a. In our study, EC-OC optical correction of charring was performed by transmittance measurements using a laser beam with a wavelength of 678 nm before and during the analysis. Transmission decreases while OC chars (in the He-mode) and increases again as pyrolytic carbon and EC release in the He/O_2-mode and the point at which the transmission reaches the pre-pyrolysis value is used as a split point to separate OC and EC (Cavalli et al., 2010). A high-performance anion-exchange chromatography–mass spectrometry (HPAEC-MS) method with an electron spray ionization technique and a quadrupole mass analyzer (Dionex ICS-3000 - Dionex MSQ™) was used for the determination of monosaccharide anhydrides (levoglucosan, mannosan, and galactosan) at m/z 161. The method used is the same as described in Saarnio et al. (2013), except that the internal standard used in this study was methyl-β-D-arabinopyranoside.

The blank filter averages were subtracted from the measurement results of the samples and the resulting values below the detection limits (DL) were assigned the values of DL/2 for further data analysis. At the traffic site and the UGA site, 25 and 22 nickel results and 14 and 10 chromium results were below the DL, respectively. For Co and Al there were altogether 8–9 results below the respective DL, while for Na^+, Mg^{2+}, Cl^-, mannosan, and galactosan there were 2–4 results below the respective DL.

The wind data measured at the UGA site was used in this study. However, it was disturbed by the effects of surrounding urban environment, e.g., buildings and trees. The average daily wind velocities at the sites during the measurement days were low, mostly below 2 m/s, which also increased the uncertainty of the wind measurements because in low wind conditions wind directions may fluctuate widely.

Boundary layer heights for Hanoi were extracted from operational forecasts of the European Center for Medium-range Weather Forecasts (ECMWF) using a regular 0.2-degree grid. The values at neighboring mesh-points were interpolated to the respective sites in Hanoi. Forecasts starting at 00 UTC were used, and the steps +06 and + 18 h (0100 and 1300 Local time) were taken for nocturnal and daytime values.

2.3. Reconstructed mass and organic matter

The reconstructed mass (RM) presents the analyzed fraction of $PM_{2.5}$ mass, which was calculated as a sum of organic matter (OM), soot (EC), secondary inorganic aerosol (SIA, as a sum of ammonium, nitrate, and sulphate), soil minerals, sea salt and the rest of elements. Geological soil minerals were calculated based on the formula by Chow et al. (2015) and Pant et al. (2015):

$$\text{Geological minerals} = 2.2\text{Al} + 2.49\text{Si} + 1.63\text{Ca} + 1.94\text{Ti} + 2.42\text{Fe}$$

However, it should be noted that neither silicon (Si), which is one of the major soil elements, nor titanium (Ti) were analyzed in this study. Additionally, calcium mass was calculated from the water-soluble fraction (Ca^{2+}) analyzed by IC which also leads to an underestimation of crustal materials. Sea salt mass was calculated from sodium as 2.54Na^+.

The share of OC originating from biomass burning was calculated from the potassium concentration as $K^+ \times 335.4/50$ based on emission factors calculated from measurements of open field rice straw burning in Thailand (Kim Oanh et al., 2011). In this study, the mass of OC from biomass burning was further converted to OM using the factor 1.9 (OM-Biomass) while the factor 1.4 was used for the rest of the OC (OM other). It should be noted that the conversion factor is generally one of the critical factors affecting the uncertainty of OM and reconstructed mass. In literature, various conversion factors have been used, e.g., Turpin and Lim (2001) suggested a factor 1.6 ± 0.2 for urban aerosol, a factor 2.1 ± 0.2 for non-urban, and even higher values for aged biomass burning aerosol (Diapouli et al., 2014).

2.4. Backward trajectories

For selected days, NOAA's Hybrid Single-Particle Lagrangian Integrated Trajectory (HYSPLIT) model (Stein et al., 2015; Rolph et al., 2017) was used to draw 72 h backward air mass trajectories based on the global meteorological data from the Global Data Assimilation System (GDAS) archive starting at 7 a.m. (00:00 UTC) with a 6 h time resolution at the site coordinates and the height of 500 m.

2.5. Fire hot spots

To study the effect of field fires on Hanoi $PM_{2.5}$ pollution, the number of fire hotspots was counted for three different domains: 1. The Red River Delta domain 210 km × 200 km around Hanoi, 2. The Northern Vietnam domain 635 km × 470 km and 3. The Northern Vietnam and South China domain 915 km × 650 km (Fig. S2). The number of fire hotspots for each measurement day was retrieved from daily Himawari satellite data. The Himawari geostationary satellite is managed by Japan Meteorological Agency and the spatial and temporal resolution of the data is 2 km and 10 min.

2.6. Source apportionment

Receptor models are used to identify air pollution sources by using measured time series of existing air pollutants and the knowledge of studied pollutants and their behavior in the atmosphere. The positive matrix factorization (PMF) model is widely used for ambient air quality research across the world (Hopke, 2016; Hopke et al., 2020).

The PMF factor analysis method is based on an uncertainty-weighted receptor model that decomposes a large number of variables in a complex data set into two matrices, i.e., factor contributions and factor profiles (Paatero and Tapper, 1994; Paatero, 1997). PMF resolves the chemical mass balance equation to find a user defined number of factors (sources) and the user selects the most realistic model solution. Traditionally, PMF has been used for source apportionment of particulate matter mass, e.g., PM_{10} and $PM_{2.5}$ (e.g., Almeida et al., 2020), but it has also been applied to combinations of species measured from different phases like PM and gases or to measurements of different time resolutions (e.g., Kyllönen et al., 2020; Belis et al., 2013; Srivastava et al., 2021; Crippa et al., 2014; Vestenius et al., 2011), particle number size distributions (e.g., Squizzato et al., 2019) and volatile organic compounds (e.g., Vestenius et al., 2011, 2021). In this study, pollution sources and their contribution to the $PM_{2.5}$ concentration in Hanoi were studied using EPA's SPECIATE 5.2 (U.S. EPA, 2013, https://www.epa.gov/air-emissions-modeling/speciate), and the chemical profiles of emission sources in Asia measured in previous studies (e.g. Kim Oanh et al., 2010, 2011).

As the number of samples was quite limited, two data sets (the traffic and UGA site) were combined to get a more representative amount of data by including the time series of first site right after the other. Thus, no averaging was performed to create this artificial 2-year dataset. An attempt was made to run PMF for each data set separately, however, we suggest that the combination solution gave the more representative results. Five days with exceptionally high Zn concentrations (>5 μg m^{-3}) at the traffic station (see 3.1.3.), and three samples at the UGA site with abnormal high elemental concentrations were excluded from the analysis. The $PM_{2.5}$ filter data (ions, trace elements, EC, OC, levoglucosan, $PM_{2.5}$ resolved mass) together with the daily averaged gas monitor data (NO, NO_2, and CO) from the NCEM and Hanoi EPA air quality stations were also used as input data for the PMF 5.0 model (Norris et al., 2014).

3. Results and discussion

The average concentrations of $PM_{2.5}$ mass and different species during the whole one-year measurement period (August 6, 2019–August 6, 2020) and separately in winter (November–March), summer (May–September), and the transition seasons of autumn (October) and spring (April) are presented in Table 1. In Hanoi the concentrations in general were higher in winter and lower in summer. The seasonal variation in Hanoi is firstly attributed to meteorological conditions. The highest $PM_{2.5}$ mass concentrations were measured on days with low nocturnal boundary layer heights, and calm winds when atmospheric dispersion had been limited (Fig. 1). The same phenomenon has also been found in earlier studies (Hien et al., 2002; Kim Oanh et al., 2006; Hai and Kim Oanh, 2013). Hanoi features a subtropical monsoon climate, and in winter the area is under the influence of the Northeast Monsoon carrying air pollutants from north-eastern Vietnam and south-eastern China (Hien et al., 2021; Hai and Kim Oanh, 2013). Earlier studies have found that black carbon (BC) enhances haze formation by inducing inversion because the top of the polluted air layer containing BC aerosols warms up more than the air closest to the earth's surface which further reduces mixing with the cleaner air aloft (Ding et al., 2016). As sunlight does not warm the earth's surface and there is less turbulence, the polluted air layer becomes even more stable and thick, causing the concentrations to increase even more (Petäjä et al., 2016). In summer, south-easterly winds carry cleaner marine air from the Gulf of Tonkin and the Pacific Ocean, and effective atmospheric dispersion and wet removal lead to declined concentrations. Dry weather during winter also enhances emissions from open biomass burning and road dust resuspension which are extensively discussed further in this paper.

The spring data showed the effect of the COVID-19 restrictions as a national lockdown was implemented in Vietnam between 1 and April 15, 2020, which was later extended until the end of April in Hanoi and some other higher risk areas (Vuong et al., 2021). In this study, only two filter samples at the UGA site and six samples at the NCEM traffic site were collected in April 2020 (Table 2). During the lockdown, schools, shopping malls and restaurants were closed, public transportation was stopped, and travel restrictions were implemented, and hence the concentrations of air pollutants in Hanoi were lower than normally found in other studies (Vuong et al., 2021; Nguyen et al., 2021). The effect of the COVID-19 restrictions could be seen also in our data as the EC concentrations at the traffic site in April were considerably lower than in winter while the levels at the UGA site were quite similar between winter and spring. Additionally, air quality in Vietnam was likely also affected by the restrictions of neighboring countries, e.g., in China nearly one-third of the cities were in lockdown during several weeks in January and February 2020 when transportation was largely banned, which improved local air quality (He et al., 2020; Yuan et al., 2021). This likely decreased the long-range transportation air pollution from China to the neighboring countries.

3.1. $PM_{2.5}$ mass and chemical composition

The average $PM_{2.5}$ concentrations of the entire one-year measurement period determined by the gravimetric method were 49 and 46 μg m^{-3} at the traffic and UGA sites, respectively (n = 118 and 99, Table 2). The national technical regulation of ambient air quality in Vietnam (QCVN 05, 2013) specifies $PM_{2.5}$ limit values as 50 μg m^{-3} and 25 μg m^{-3} for 24-h and annual average, respectively, and the latest WHO air quality guidelines (AQGs) set for $PM_{2.5}$ are 15 and 5 μg m^{-3}, for 24-h and annual average, respectively (WHO, 2021a). The measured $PM_{2.5}$ annual averages in Hanoi were about twice the national limit value and 9–10 times higher than the 2021 WHO AQG. The WHO annual interim target 1 of 35 μg m^{-3} (WHO, 2021a) was exceeded as well. From August to September 2019, and from May to August 2020, daily $PM_{2.5}$ concentrations remained below the Vietnam 24-h NAAQS, but during the winter months the NAAQS was frequently exceeded at both sites. Noticeably, concentrations over 100 μg m^{-3} were measured on nine days at the traffic site and on four days at the UGA site in winter (Fig. S3). The highest $PM_{2.5}$ monthly average was measured in December: 93 μg m^{-3} at the traffic site and 76 μg m^{-3} at the UGA site. Strong seasonal variation and high concentrations of pollutants during

Table 1
Average concentrations and standard deviations (SD) of daily concentrations of $PM_{2.5}$ weighed mass (W) (only those samples that were taken to chemical analysis), resolved mass (RM) and chemical compounds in $PM_{2.5}$ in Hanoi in 2019–2020 and in different seasons: summer: August–September 2019 & May–August 2020, winter: November 2019–March 2020, autumn: October, spring: April (COVID-19 restrictions in Hanoi). N = number of samples. The traffic site (NCEM) and the UGA site (Hanoi EPA).

	NCEM		Hanoi EPA		NCEM		Hanoi EPA		NCEM		Hanoi EPA		NCEM		Hanoi EPA		NCEM		Hanoi EPA	
	All		All		Autumn		Autumn		Winter		Winter		Spring		Spring		Summer		Summer	
	Average	SD	Average	SD	Average	SD	Average	SD	Average	SD	Average	SD	Average	SD	Average	SD	Average	SD	Average	SD
W μg m^{-3}	55[a]	40	48[b]	38	64	17	45	12	76[a]	49	64	50	50	23	53	24	33[a]	14	31[b]	13
RM μg m^{-3}	38	24	32	21	56	10	39	8	47	31	39	28	24	11	31	17	29	14	26	13
Na^+ μg m^{-3}	0.17	0.08	0.15	0.08	0.06	0.06	0.21	0.10	0.19	0.09	0.17	0.10	0.08	0.03	0.13	0.01	0.15	0.06	0.13	0.05
NH_4^+ μg m^{-3}	2.53	1.95	2.72	2.01	3.48	2.05	3.20	1.54	3.31	2.35	3.59	2.49	2.35	1.60	2.75	1.10	1.66	1.03	1.86	1.15
K^+ μg m^{-3}	0.51	0.35	0.54	0.39	0.68	0.20	0.60	0.16	0.55	0.41	0.58	0.46	0.30	0.13	0.45	0.19	0.47	0.32	0.50	0.36
Mg^{2+} μg m^{-3}	0.04	0.03	0.04	0.02	0.07	0.03	0.06	0.02	0.05	0.04	0.04	0.03	0.02	0.01	0.04	0.03	0.04	0.03	0.03	0.01
Ca^{2+} μg m^{-3}	0.23	0.15	0.23	0.13	0.36	0.09	0.29	0.15	0.27	0.04	0.23	0.16	0.09	0.07	0.19	0.22	0.19	0.11	0.22	0.09
Cl^- μg m^{-3}	0.84	1.05	0.47	0.67	1.80	1.74	0.60	0.37	1.33	0.16	0.82	0.83	0.41	0.27	0.46	0.14	0.29	0.41	0.14	0.32
NO_3^- μg m^{-3}	2.91	3.11	2.74	3.52	4.65	1.50	3.53	2.64	4.66	1.14	4.73	4.43	3.10	2.72	2.42	1.19	0.94	1.20	0.85	0.79
SO_4^{2-} μg m^{-3}	6.11	3.85	6.28	3.80	9.75	3.42	8.55	2.54	6.46	4.43	6.60	4.11	4.83	2.63	6.99	3.80	5.39	3.16	5.59	3.63
OC μg m^{-3}	11.6	8.7	10.3	7.6	14.6	3.1	10.5	3.2	15.1	11.5	12.6	10.2	6.3	3.2	8.9	5.4	8.6	4.5	8.4	4.5
EC μg m^{-3}	3.56	1.57	1.80	0.87	4.97	1.99	2.58	1.01	3.45	1.57	1.83	0.88	1.74	0.54	1.80	0.85	3.74	1.34	1.65	0.81
Levo[c] μg m^{-3}	0.43	0.38	0.38	0.35	0.52	0.15	0.39	0.15	0.54	0.48	0.45	0.42	0.24	0.08	0.39	0.12	0.33	0.28	0.30	0.30
Al ng m^{-3}	179	129	168	118	254	86	234	149	225	146	185	144	76	46	182	164	140	102	141	75
As ng m^{-3}	5.31	3.47	4.94	3.06	9.04	3.19	6.67	2.86	5.86	4.11	5.35	3.58	3.49	2.13	5.57	3.79	4.46	2.41	4.24	2.46
Cd ng m^{-3}	4.02	5.27	2.31	2.32	7.31	4.30	4.93	4.64	4.18	4.76	2.38	1.94	2.17	1.88	2.33	1.26	3.64	6.10	1.82	1.93
Co ng m^{-3}	0.16	0.16	0.12	0.08	0.32	0.32	0.18	0.05	0.17	0.12	0.13	0.09	0.09	0.05	0.13	0.06	0.13	0.15	0.10	0.07
Cr ng m^{-3}	3.97	6.98	2.79	2.75	5.33	1.43	3.62	1.46	3.75	3.05	3.40	3.78	1.23	0.87	2.64	0.57	4.40	10.09	2.11	1.47
Cu ng m^{-3}	18	18	18	33	35	35	25	17	18	13	14	12	9	7	19	19	18	19	21	45
Fe ng m^{-3}	271	185	215	156	398	63	293	98	316	204	234	154	166	73	265	45	226	173	183	164
Mn ng m^{-3}	47	51	33	29	88	52	61	34	45	53	34	30	24	22	45	3	45	51	27	26
Ni ng m^{-3}	1.40	1.20	1.27	1.45	2.52	0.78	1.72	0.39	1.72	1.42	1.67	2.05	0.36	0.16	0.52	0.32	1.10	0.87	0.88	0.63
Pb ng m^{-3}	185	233	87	90	234	174	144	79	206	257	86	73	81	68	95	20	175	234	79	105
V ng m^{-3}	1.39	0.84	1.36	0.89	2.07	0.71	2.49	1.35	1.41	0.98	1.20	0.71	0.64	0.38	0.82	0.31	1.38	0.67	1.35	0.85
Zn ng m^{-3}	1835	2956	753	988	4539	6264	1490	1242	2013	3158	746	1098	1188	1680	865	832	1325	1787	635	823
N samples	82		78		6		6		34		33		6		2		36		37	

[a] NCEM Resolved mass N = 76, winter N = 33, summer N = 32.
[b] Hanoi EPA Resolved mass N = 73, summer N = 32.
[c] Levoglucosan.

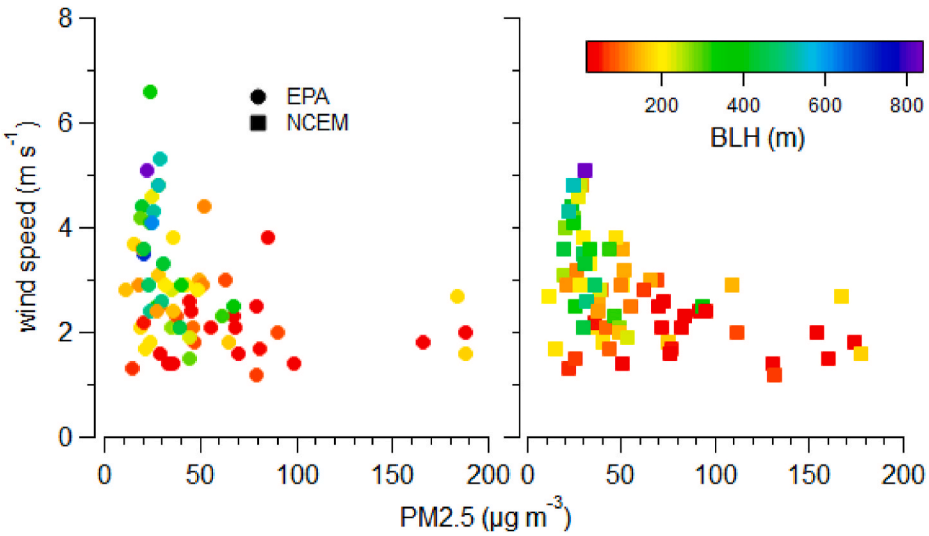

Fig. 1. Wind speed (at Noi Bai airport, Hanoi) as a function of weighed $PM_{2.5}$ mass at the NCEM traffic site and the Hanoi EPA UGA site. Boundary layer height (BLH) at night at 1:00 a.m. is expressed using a color scale.

Table 2
Monthly average concentrations, standard deviations (SD) and number of sample days (N) of $PM_{2.5}$ weighed mass (W) and resolved mass (RM) in Hanoi in 2019–2020. The traffic site (NCEM) and the UGA site (Hanoi EPA).

	NCEM $PM_{2.5}$			Hanoi EPA $PM_{2.5}$			Hanoi EPA $PM_{2.5}$			NCEM $PM_{2.5}$			EPA $PM_{2.5}$		
	Weighed μg m^{-3}	SD	N	Weighed μg m^{-3}	SD	N	Monitor μg m^{-3}	SD	N	RM μg m^{-3}	SD	N	RM μg m^{-3}	SD	N
Aug 2019	30	11	7	14	3	3	37	12	26	36	10	9	26	10	10
Sep 2019	39	22	11	44	23	9	49	20	30	38	17	10	36	15	9
Oct 2019	51	23	11	40	15	8	43	17	31	56	10	6	39	8	6
Nov 2019	69	34	11	59	29	9	66	26	30	66	27	7	48	22	7
Dec 2019	93	54	11	76	57	10	74	36	31	68	34	8	54	34	7
Jan 2020	72	53	6	74	58	7	51	31	31	40	25	5	38	30	5
Feb 2020	58	44	10	58	49	10	69	46	29	33	26	7	35	30	7
Mar 2020	42	23	10	31	10	9	50	22	31	24	12	7	19	7	7
Apr 2020	42	20	12	50	18	3	45	23	30	24	11	6	31	17	2
May 2020	30	6	11	32	7	8	41	11	31	19	6	6	18	4	6
Jun 2020	32	10	7	33	11	10	33	14	29	22	10	6	20	10	6
Jun 2020	28	6	8	29	10	10	28	17	31	18	6	5	22	16	6
Aug 2020	26	2	3	25	7	3	26	10	6						
Annual	49	34	118	46	35	99	48	28	366	38	24	82	32	21	78

the dry season from October to January have similarly been found in earlier studies in Hanoi (Cohen et al., 2010a; Hien et al., 2021). The average concentrations of $PM_{2.5}$ mass and chemical compounds are compared to some other urban sites with higher concentration levels, e.g., Wuhan and New Delhi, and sites with lower $PM_{2.5}$ levels compared to Hanoi like Seoul and Krakow in Table S1. The $PM_{2.5}$ mass concentration level in this study was close to that measured in Beijing in 2019, although the chemical composition was different (Table 1S).

The $PM_{2.5}$ reconstructed mass (RM, see section 2.3.), was calculated as a sum of OM, EC, SIA, soil minerals, sea salt and the remaining elements (Fig. 2.). The average RM was 38.2 ± 24.3 μg m^{-3} at the traffic site (n = 82) and 32.4 ± 21.2 μg m^{-3} at the UGA site (n = 78). Thus, considering the averages of weighed mass, 71% and 69% of the mass at the traffic (n = 76) and UGA site (n = 73) were explained by these

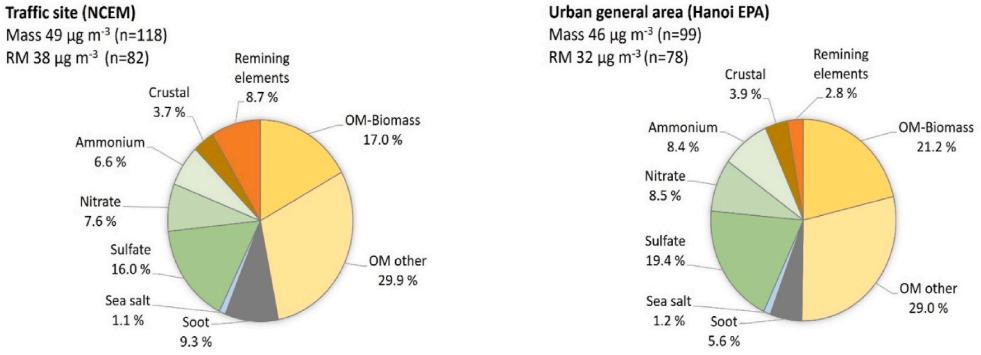

Fig. 2. $PM_{2.5}$ reconstructed mass (RM) and chemical composition.

reconstructed mass groups, respectively. About half of the RM was OM, 30–36% was SIA, 6–9% EC, 4% soil minerals, 1% sea-salt and the remaining 3–9% trace elements. It is likely that a portion of volatile compounds, e.g., ammonium nitrate and volatile organic compounds may have evaporated during the 24-h sampling, transportation and storage, although the samples were stored refrigerated (+5 °C) until analysis. More detailed results of the main analyzed components are presented below in sections 3.1.1.-3.1.5.

3.1.1. Organic compounds and elemental carbon

Organic compounds had the strongest impact on the measured $PM_{2.5}$ mass in Hanoi throughout the measurement period and OM dominated in all seasons. The average concentrations of OC were similar at both sites (Table 1). OM was calculated from OC (see 2.3) and it was 18.3 and 16.3 μg m^{-3} at the traffic and UGA site, respectively. OM was at the same level as in the previous studies in Hanoi (Cohen et al., 2010a; Hai and Kim Oanh, 2013). There was a high seasonal variation: in winter, concentrations were considerably higher than in summer. From October to December 2019 there were days with increased $PM_{2.5}$, OM, K^+ and levoglucosan concentrations. Levoglucosan and potassium can be treated as tracers for biomass burning (see 3.1.4 and 3.3), although potassium has also other sources. As the correlations between potassium and levoglucosan were high (Pearson $r^2 = 0.91$ at the traffic and $r^2 = 0.89$ the UGA site), it was assumed that the main source of potassium was biomass burning and potassium was used for estimating the OC concentration originating from biomass burning (see section 2.3). Accordingly, 36% and 42% of OM at the traffic and UGA sites originated from biomass burning. The traces of biomass burning, potassium and sugar anhydrides, will be discussed later in section 3.4.

Concentrations of EC were about two times higher at the traffic site (3.6 ± 1.6 μg m^{-3}) than at the UGA site (1.8 ± 0.9 μg m^{-3}), which was expected as traffic is an important source of EC (Table 1). Similar EC concentrations (2.7 μg m^{-3}) have been measured in Hanoi (Hai and Kim Oanh, 2013). However, during the COVID-19 restrictions in April 2020, the EC concentrations at the traffic site dropped to about the same level (1.7 μg m^{-3}, n = 6) as the UGA site average (1.8 μg m^{-3}). At both sites the EC levels were the highest in October, but the UGA site generally did not exhibit significant seasonal variation (Fig. 3). At the traffic site, EC concentrations were higher during the first half of the measurement period, decreased in January 2020 and stayed at a lower level till the end of the measurement period, i.e., the end of July 2021.

The average OC/EC ratio was lower at the traffic site (3.2) than at the UGA site (5.7). Both values were higher than the ratios 0.8–1.4 typically found at traffic sites (Lee et al., 2006; Tao et al., 2012) or the ratio 2.7 found for coal combustion by Watson and Chow (2001). The average OC/EC ratio 5.7 at the UGA site was at the same level as that measured in the smoke of rice straw open burning (5.7, Kim Oanh et al., 2011) indicating a high influence of biomass burning and/or aged aerosol. In addition to open agricultural fires and domestic solid waste open burning, residential biomass combustion using agricultural residues, fuel wood, and honeycomb coal briquettes (consisting of a mixture of anthracite particles, mud, peat, etc.) for cooking in Northern Vietnam (Huy et al., 2021) may have increased the OC/EC ratio. Additionally, an important factor for increasing the OM in $PM_{2.5}$ is the formation of secondary organic aerosol (SOA) in photochemical reactions of NOx and volatile organic compounds (VOCs) emitted from anthropogenic (like traffic and industry, biomass and coal combustion) and biogenic sources.

The concentration of OC and EC in Hanoi were higher than those measured in Beijing and Seoul, but OC was at about the same level as in Wuhan (Table S1). However, in New Delhi OC and EC concentrations

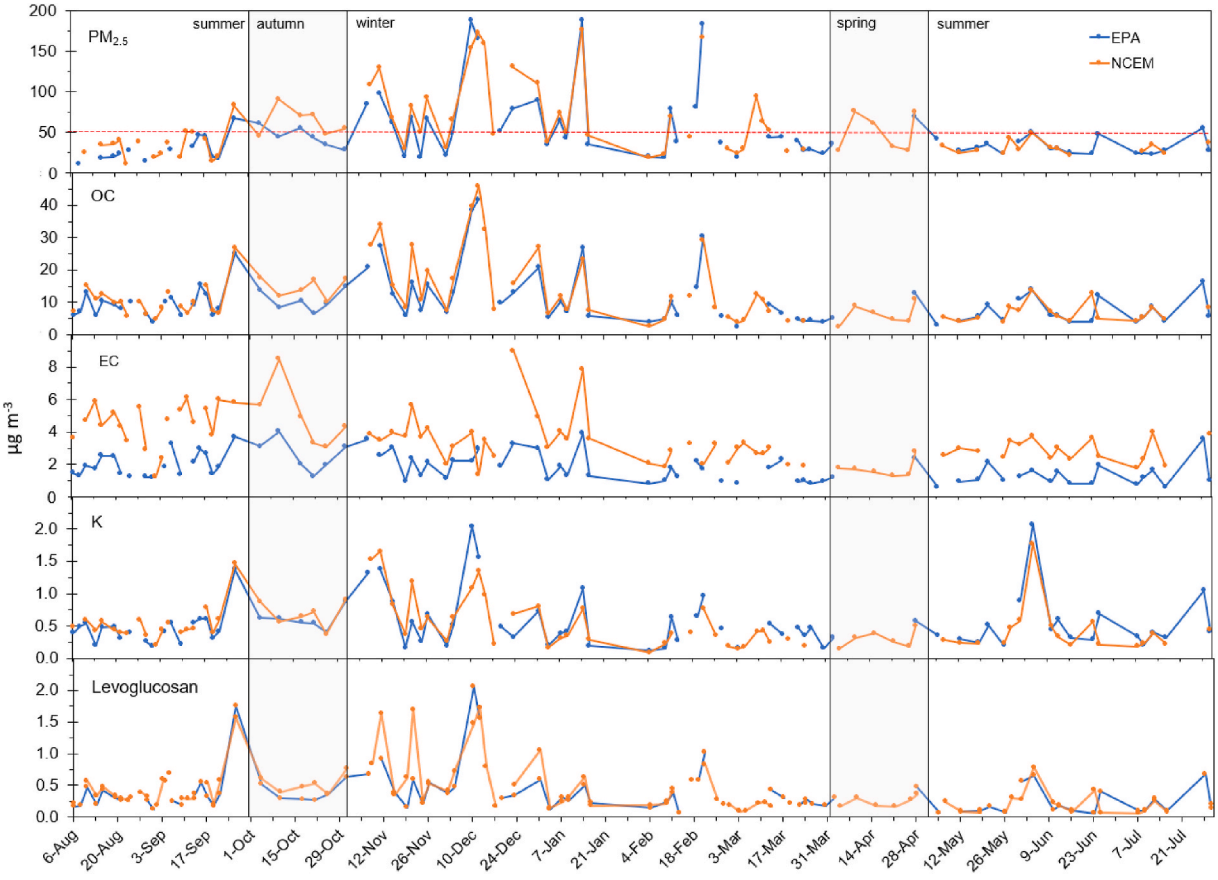

Fig. 3. The $PM_{2.5}$, OC, EC, potassium, and levoglucosan concentrations measured at the traffic site (NCEM) and the UGA site (Hanoi EPA) in Hanoi August 8, 2019–July 30, 2020. The Vietnamese annual average limit value for $PM_{2.5}$ (50 μg m^{-3}) is marked with the red line.

were even higher than in Hanoi (Table S1).

3.1.2. Water-soluble ions

About one third of the reconstructed mass was SIA, including ammonium, sulphate, and nitrate, that is 30% (11.6 ± 8.1 μg m^{-3}) and 36% (11.7 ± 8.4 μg m^{-3}) at the traffic and UGA sites, respectively (Table 1). SIA is formed in ambient air from their precursor gases of sulfur dioxide, nitrogen oxides and ammonia. The abundance of the main ions was the following: $SO_4^{2-} > NO_3^- > NH_4^+ \gg Cl^-$, $K^+ > Ca^{2+} > Na^+ > Mg^{2+}$ (Table 1). Of the water-soluble SIA, sulphate dominated followed by nitrate, indicating a strong contribution of fossil fuel combustion, e.g., coal and oil combustion. In Northern Vietnam, the coal-fired thermal power plants in Hai Phong and Quang Ninh Provinces are large stationary sources emitting SO_2 and NOx. In Hanoi city, traffic is considered the main source for NOx, precursor gases of nitrate, but it is also emitted from power plants and industries. Major ammonia sources are related to agricultural activities, but it is also released from biomass burning, sewage works, and waste handling (Sutton et al., 2000; Xu et al., 2018). Ammonium nitrate has temperature dependent equilibrium state in air, and in warm conditions it decomposes to gaseous ammonia and nitric acid (Nowak et al., 2010), which may be one reason for lower NH_4NO_3 concentrations in summer. In addition, volatile losses during sampling in the warm season are expected to be remarkable. In general, SIAs at the two sites were in a similar range and had a similar temporal variation pattern with the highest concentrations in October and winter which decreased towards the summer in 2020 (Fig. 4). In this study, the sulphate concentrations were lower than those reported by previous studies (9–18 μg m^{-3}) in Hanoi (Cohen et al., 2010a; Kim Oanh et al., 2006; and Hien et al., 2021).

Based on the ion balance calculations the aerosol was close to neutral, namely, 0.95 (slightly acidic) and 1.04 (slightly alkaline) at the traffic and UGA sites, respectively. However, there was some temporal variation: until 7 May the ion balance was mainly neutral except for a couple of acidic samples, but during the rest of the study period the ion balance was basic. The found ammonium excess may indicate the spreading of manure or N-fertilizers for vegetation planting. The four exceptional, acidic traffic site samples with chloride excess and high zinc and lead contribution are discussed later in section 3.4.

The average Ca^{2+} concentration was 0.23 μg m^{-3} at both sites and the highest concentrations occurred from October to December. In addition to Ca^{2+} originated from resuspended soil dust and construction dust which are more intensive during the dry season, this species is emitted from industrial sources, e.g., cement production. Na^+ concentrations were low indicating a low contribution of sea salt, about 1% of RM at both sites. Usually, sea salt Cl^- is replaced by NO_3^- during transportation from the seaside (Pathak et al., 2003). However, the measured chloride concentrations were higher than expected for solely sea salt origin, especially at the traffic site. The Cl^- to Na^+ molar concentration ratios at the traffic (7.8) and the UGA sites (4.7) were higher compared to the common ratio in sea water (1.8) indicating an effect of anthropogenic sources which affected the traffic site more. In China, high Cl^- concentrations and high Cl^- to Na^+ mass ratios (2.46–5.00) measured at polluted sites have been found to indicate coal combustion and biomass burning. Similarly, in Hong Kong, elevated non-sea salt Cl^- concentrations have been found when air masses arrived from China (Yang et al., 2018). Kim Oanh et al. (2011) reported about 7% of Cl^- in

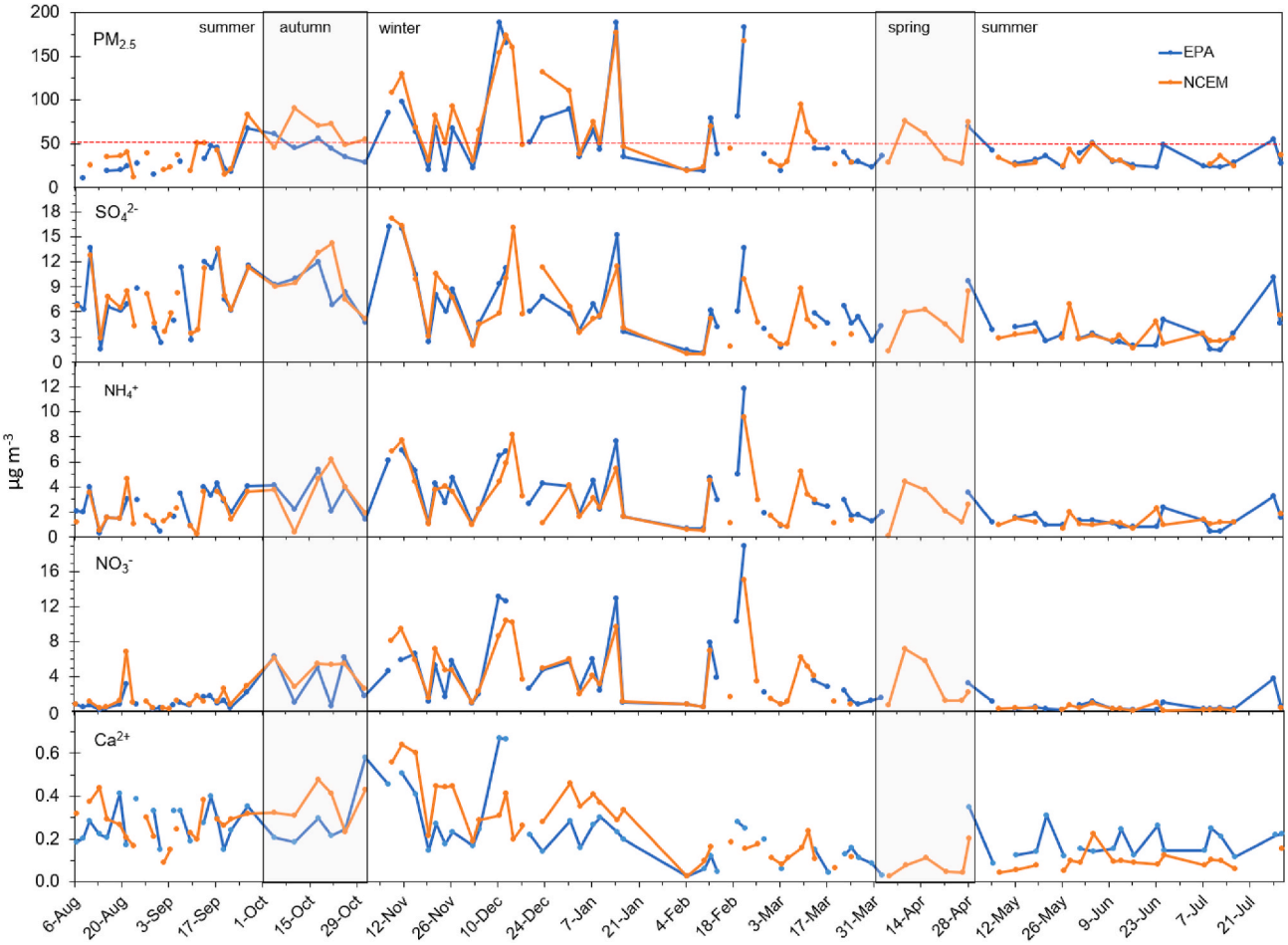

Fig. 4. Concentrations of $PM_{2.5}$ mass, SO_4^{2-}, NO_3, NH_4^+ and Ca^{2+} at the traffic site (NCEM) and the UGA site (Hanoi EPA) in Hanoi August 8, 2019–July 30, 2020. The Vietnam 24 h NAAQS for $PM_{2.5}$ (50 μg m^{-3}) is marked with the dotted red line.

$PM_{2.5}$ to be emitted from rice straw field burning.

The Hanoi sulphate concentrations were two times higher than nitrate concentrations, at the same level as in Beijing (Table S1), indicating a higher contribution of fossil fuel consumption. However, sea salt and ammonium nitrate concentrations in Hanoi were lower compared to some other Asian sites (Table S1).

3.1.3. Crustal and trace elements

Crustal elements mostly originate from soil, road dust and construction work and a major part of them exist as coarse particles (>2.5 μm). Principally, Silicon (Si) is the major crustal element; however, it was not measured in this study. The average shares of crustal elements in RM, estimated from Al, Ca, and Fe concentrations, were roughly 1% at both sites, and, as expected, the concentrations of Al, Fe and Mn were higher at the traffic site than at the UGA site because of the influence of resuspension of road dust (Table 1). The shares of remaining elements (including potassium, which is discussed in section 3.1.4.) in RM were 8.7% and 2.8% at the traffic and UGA sites, respectively. The higher share of trace elements at the traffic site was caused by high Zn concentrations. At both sites the abundance of the elements from the most significant was the following: Zn » Fe > Pb > Al > Mn > Cu > As > Cd > Cr > Ni > V > Co. Typically, the concentrations of trace elements were higher at the traffic site compared to the UGA site except for copper, which did not differ between the sites and vanadium which was often higher at the UGA site. Copper mainly originates from non-ferrous industrial sources whereas V and similarly Ni, are typically emitted from heavy oil refineries, fuel oil and coal combustion (WHO, 2000).

The annual average concentrations of Pb, Cd, As, and Ni measured in this study did not exceed the WHO AQGs or national standard values. The WHO annual AQG value for Pb in PM_{10} is the same as the annual limit value of Vietnam, 0.5 μg m^{-3}. The Pb annual average in $PM_{2.5}$ at the traffic site, 185 ± 233 ng m^{-3}, was more than twice of that at the UGA site (87 ± 90 ng m^{-3}) but with large temporal variations in daily values. Since Vietnam has phased out the use of leaded gasoline back in 2001 (WB, 2002) the higher concentrations of Pb at the traffic site were not expected to originate directly from vehicle exhaust, but rather from non-exhaust emissions (such as tire and break wear) and resuspended road dust as well as other related sources of heavy metals like solid waste open burning and the industries discussed below. Compared to the measurements conducted in 2001–2008 (Pb average 236 ng m^{-3}) in Hanoi, lead concentrations have decreased but our results were in fact higher than those reported for year 2015 (Pb average about 70 ng m^{-3}) for a general urban site by Cohen et al., (2010a) and by Hien et al. (2021).

The measured annual average concentrations of Cd (Table 1) were below the annual WHO AQG value in PM_{10} (5 ng m^{-3}, WHO, 2000). At the traffic site, daily Cd concentrations were often higher than at the UGA site and were frequently over 5 ng m^{-3} from August to December. In the spring, however, the concentrations were low. It should be noted that in this study these elements were measured in the $PM_{2.5}$ and not in the PM_{10} fraction, and therefore we cannot conclude that the above mentioned WHO AQGs would not have been exceeded if the heavy metals had been measured from PM_{10}. Nevertheless, more than 80% of Pb, Cd, As and Ni have earlier been found in the fine fraction (e.g., Makkonen et al., 2010). Typical cadmium sources are coal combustion, industrial processes, and waste burning (Pacyna et al., 2009).

The WHO has not set any AQG for As or Ni. However, India has set an air quality annual standard value of 6 ng m^{-3} for As and 20 ng m^{-3} for Ni in PM_{10} (India, 2009). These values are also considered as annual target values in the EU (EU, 2004). The measured annual averages for As and Ni were below these air quality standards (Table 1). Daily As and Ni concentrations were mainly higher in autumn and winter and lower in spring, possibly partly due to the COVID-19 restrictions. All the measured Ni concentrations in Hanoi were low (Table 1) and from April until July 2020 were close to the detection limit.

The average concentrations of soil elements, e.g., Fe and Al, were lower in Hanoi than in Wuhan and New Delhi where soil elements dominated (Table S1). In Hanoi, Zn was the major element with much higher concentrations than in Wuhan and New Delhi. Of the elements typical for coal combustion, the As concentration was much lower in Hanoi than in Wuhan, but interestingly, the Pb and Mn concentrations were higher (Table S1).

3.1.4. Zinc peaking high with chloride

Interestingly Zn, the most abundant trace element at both sites, occasionally, peaked high with chloride, especially at the traffic site (Fig. 5). The average Zn concentration at the traffic site was twice as high as at the UGA site (Table 1). The Zn concentrations correlated with Cl^-, Cd, Mn, EC, and Pb concentrations (Fig. S4) indicating a major industrial source, e.g., non-ferrous metal processes have been considered the largest global sources of Zn, Cd and Pb (Pacyna and Pacyna, 2001; Shiel et al., 2010). In addition, according to Huang et al. (2004), fly ash enriched in fine particles from coal power plants contains toxic elements like Zn, Pb and Cd while, hydrochloric acid is also emitted. However, the high chimneys of power plants allow spreading and dilution of the flue gas efficiently over large areas. In addition, in Hanoi honeycomb charcoal has also been used for domestic cooking, and according to an emission test performed in China (Yan et al., 2022) zinc is one major element emitted from the combustion of honeycomb charcoal. For Zn there are also other sources like waste burning, traffic (e.g., tire wear and lubricant oil), and re-emission from soil. For example, household solid waste combustion has been shown to release high concentrations of Zn and Cl^- (Timonen et al., 2021). The high Zn concentration days are further discussed in 3.4.2.

3.1.5. Potassium and sugar anhydrides

Potassium and levoglucosan (1,6-anhydro-β-D-glucopyranose) are considered tracers for biomass burning, although K^+ also has other sources like the soil, production and use of fertilizers, and sea salt. The average contribution of K^+ to RM was 1.3% (traffic site) and 1.7% (UGA site) (Table 1). In biomass burning, cellulose and hemicellulose break down forming several organic compounds including sugar anhydrides like levoglucosan, mannosan, and galactosan (Simoneit et al., 1999; Simoneit, 2002). Levoglucosan is the main biomass pyrolysis product, and therefore it is a commonly used biomass burning tracer, as the other two sugar anhydrides galactosan (1,6-anhydro-β-D-galactopyranose) and mannosan (1,6-anhydro-β-D-mannopyranose) are produced in minor quantities. The major portion of the sugar anhydrides was levoglucosan (88%), as galactosan (7%) and mannosan (5%) were found at much lower concentrations in our $PM_{2.5}$ samples (Table 1).

After exclusion of the extreme K^+ −results of two samples at the traffic site (November 8, 2019 and June 4, 2020) and one sample at the UGA site (June 4, 2020) (K^+ = 1.8–2.1 μg m^{-3}), the OC, levoglucosan and K^+ concentrations showed strong correlations between each other (r^2 = 0.82–0.91) indicating their similar sources. From mid-September 2019 until the end of February 2020, K^+ and sugar anhydride peaks appeared with OC peaks indicating a high influence of biomass burning (Fig. 3). Like the concentrations of the other species, the biomass burning tracers were higher in winter, not only because of higher emissions, but also because of more stagnant meteorological conditions. In summer, except in the beginning of June, the concentrations of OC and biomass burning tracers were small with less variation.

The ratios of levoglucosan/K^+ and levoglucosan/mannosan have commonly been used to distinguish between possible biomass burning sources. In this study, the average levoglucosan/mannosan ratios (20.7 ± 5.9 and 21.3 ± 6.6) were in the range common for both agricultural waste and fuel wood burning. The average levoglucosan/K^+ ratios of 0.82 ± 0.35 and 0.70 ± 0.33 at the NCEM and the Hanoi EPA, respectively, were at a level typical for rice straw burning (0.62 ± 0.32) according to Cheng et al. (2013). However, the ratio of levoglucosan/K^+ reported by Kim Oanh et al. (2011) for fresh $PM_{2.5}$ emitted from rice straw spread field burning was higher, 1.12. In this study, there were

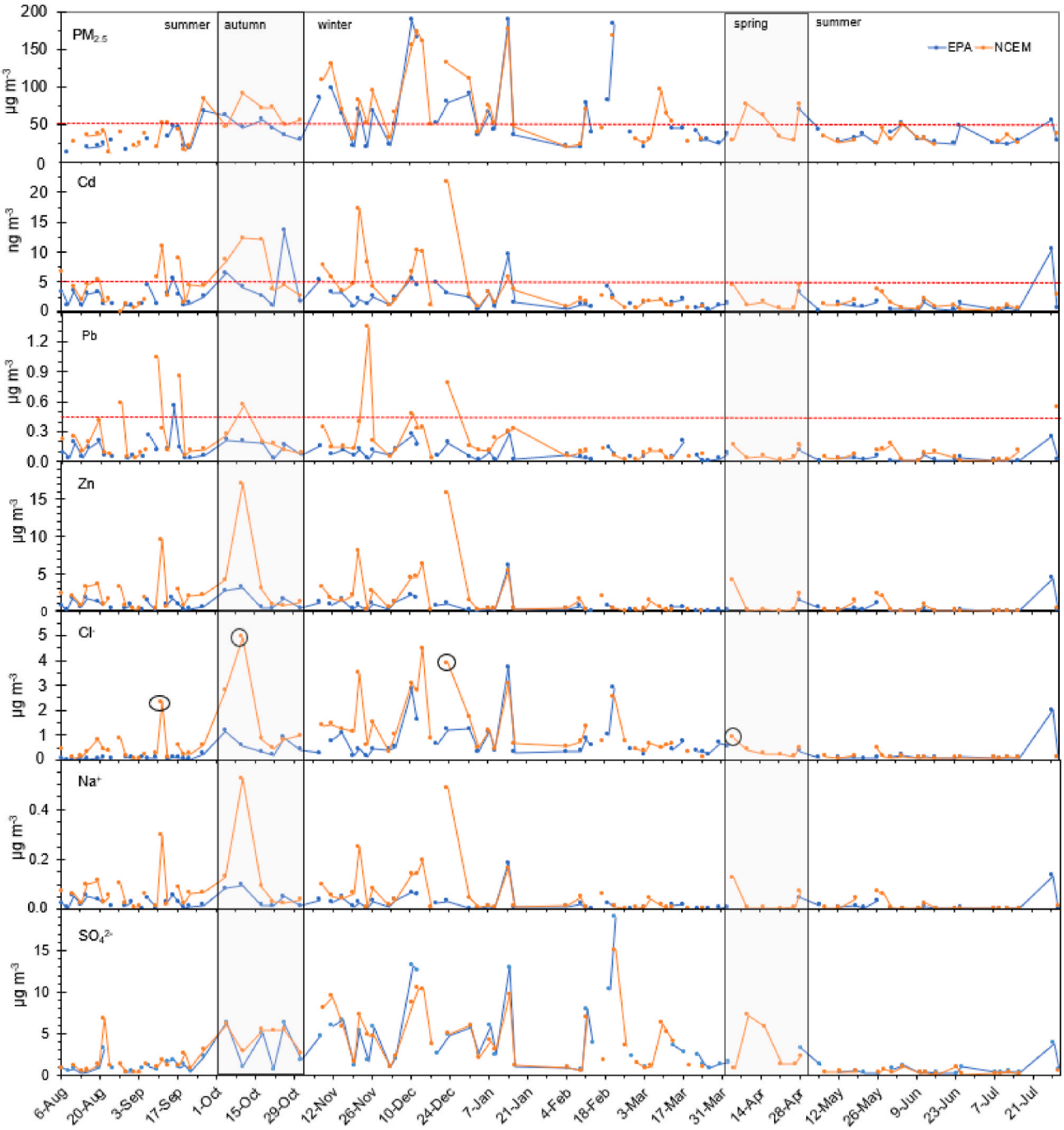

Fig. 5. Concentrations of $PM_{2.5}$ mass, Cd, Pb, Zn, Cl^-, Na^+ and SO_4^{2-} at the traffic site (NCEM) and the UGA site (Hanoi EPA) August 8, 2019–July 30, 2020. The days with Cl^- excess are marked with black circles. The Vietnam 24 h NAAQS for $PM_{2.5}$ (50 μg m^{-3}) and the WHO AQG values for Pb (0.5 μg m^{-3}) and Cd (5 ng m^{-3}) are marked with the red dotted lines.

some days with high concentrations of levoglucosan and K^+ with levoglucosan/K^+ ratios higher than 1.2 which could indicate fresh rice straw burning as well as the burning of hardwood, e.g., for domestic cooking (e.g., September 26, 2019 and February 21, 2020). On two days (November 8, 2019 and June 4, 2020) there were unusually high K^+ concentrations compared to levoglucosan and OC. On June 4, 2020, remarkably high K^+ peaks occurred at both sites, indicating a more regional source, but based on satellite observations, there were only 9 fires detected in the Red River Delta Domain, two of which were 10 km SW from Hanoi. The high contribution of K^+ on June 4, 2020 could have partly been caused by other sources such as the application of potassium fertilizers. On November 8, 2019, the K^+ concentration was high compared to levoglucosan at the traffic site and the $PM_{2.5}$ mass was also high, 108 μg m^{-3}, and several fires occurred in the Red River Delta (85 fire counts), but on the same day soil minerals and ammonium sulphate also peaked. Therefore, it is likely that also part of K^+ originated, e.g., from soil dust or fertilizers.

The levoglucosan/K^+ ratios were higher in winter with 0.97 and 0.83, compared to summer with 0.66 and 0.59, at the traffic and UGA sites, respectively. The amount of levoglucosan emitted from a fire source depends on the burning material and type of burning, e.g., in smoldering fires more levoglucosan is formed. The concentration of levoglucosan decreases sharply as the distance from the source increases, because of decomposition and fallout in atmosphere (Li et al.,

2021). In the Northern Vietnam, rice straw burning is a key local source of $PM_{2.5}$ which is more intensive in May–June and October–November each year following the harvesting activities. The contribution of this source is reflected in the PM levels and composition found in this study.

3.2. Fire hotspots

As in the other Asian countries, agricultural field burning is a common practice in Northern Vietnam to quickly clear agricultural waste after harvesting, e.g., rice and maize residue, and to prepare the land for new crop plantation. In addition, some forest and bush fires may occur on hot and windy days each year in the surrounding areas of Hanoi. Furthermore, biomass is used as fuel for cooking and small-scale open burning of municipal solid waste burning is still common in suburban areas.

To study the effect of open field agricultural fires on our results, the fire spots found in the Himawari geostationary satellite data were analyzed. Among the measurement days there were eight days with more than 100 fire counts in the Red River Delta domain (D1, Fig. S2), less than 100 km from Hanoi, and the two highest fire counts, >200, occurred on 4 and 10 December. In the Northern Vietnam (D2) and Northern Vietnam & South China domains (D3) the highest fire episodes occurred in March–April 2020. On 13 and 30 March, more than 8000 and 15 000 fire counts were found in D2 and D3, respectively. However, concentrations of K^+ and levoglucosan in all the samples collected in March remained rather low. The lifetime of levoglucosan in the atmosphere varies, being on average 1.8 days, but its contribution decreases sharply as the distance from the source increases (Li et al., 2021). Therefore, we can assume that long-range transportation, e.g., fires from the neighboring countries, does not significantly increase the levoglucosan concentrations at the measurement sites. However, in this study we did neither find K^+, nor OC peaking in March, likely because of effective atmospheric mixing. Besides, as we saw with the other pollutants, the concentrations of fire tracers were higher on the days with a low nocturnal boundary layer. K^+ and levoglucosan were occasionally high also on the days with less open field fires, which suggests the influence of domestic biomass burning for cooking and/or minor municipal waste burning in the region. There were just weak correlations (0.25–0.50) between fire counts in D1 and concentrations of $PM_{2.5}$, K^+ and levoglucosan at both sites. For the fire counts of the larger domains (D2 and D3) there was not any correlation.

It may be useful to refer to a study in China where about 74% of levoglucosan is originated from domestic biomass burning (straw, corncob, and firewood) and open biomass burning (straw, grassland, forest) (Wu et al., 2021). Although it is difficult to distinguish between open and domestic biomass burning when the same kind of agricultural residue or wood is burned, the study for China considered that 39% of formed levoglucosan originated from domestic biomass burning, 34% from open biomass burning and about 10% from municipal waste burning (Wu et al., 2021). All these sources are also important contributors to $PM_{2.5}$ pollution in Hanoi.

3.3. Source apportionment

In PMF modelling, different combinations of four to nine source factor solutions were tested. A six-factor solution was found to be the most interpretable and best explained the main sources of PM2.5 in Hanoi. The solution was validated using bootstrapping (lowest mapping of 92% for Factor 6) and displacement analysis. Factors 1 and 6 were less independent and might be slightly mixed while other factors were stable. The result of PMF analysis with six main source factors (F) affecting PM2.5 resolved mass includes: F1: Traffic, F2: local SIA (mainly NH_4NO_3), F3: biomass burning, F4: Zn–Pb related industry, F5: LRT-SIA ($(NH_4)_2SO_4$ mixed with trace elements), and F6: Dust (Fig. 6). Profiles of each source factor and their contributions are presented in the supplementary material (Fig. S5).

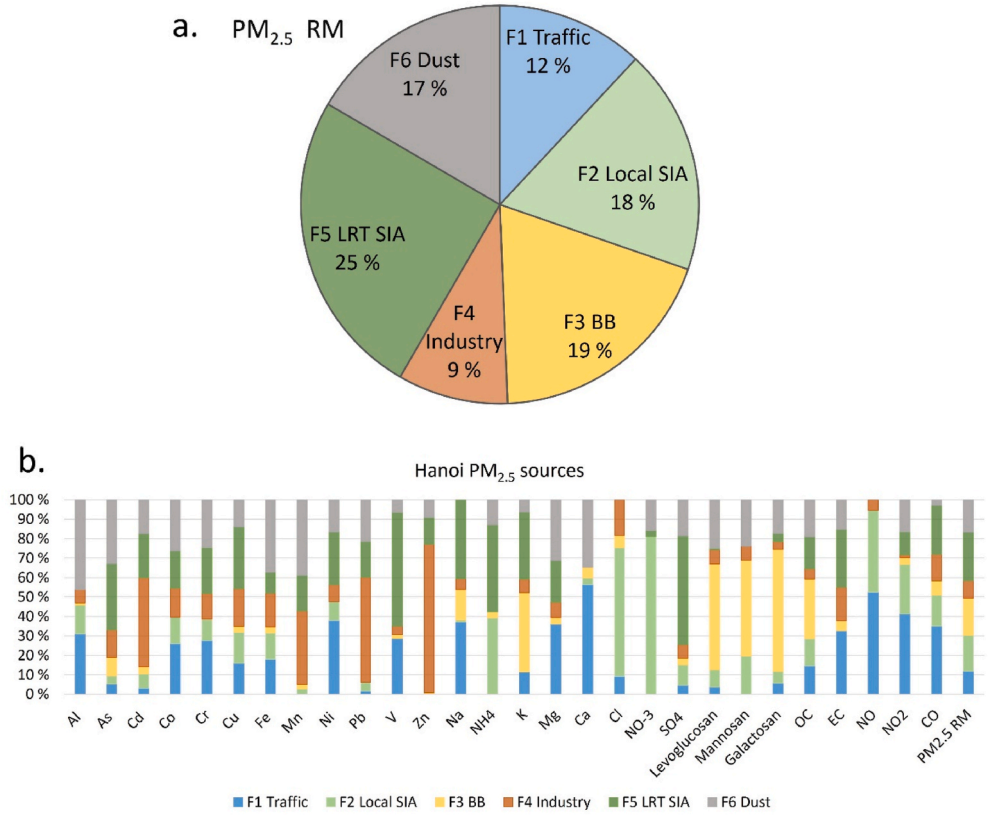

Fig. 6. The main $PM_{2.5}$ sources at Hanoi and their contribution to $PM_{2.5}$ resolved mass (a.), and contribution of each species to different factors (b.).

Factor 1 consisted mainly of traffic emissions NO (53% of compound mass), NO_2 (41%), CO (35%), EC (33%) and OC (15%) and resuspended road dust (Al 31% and Ca 56%). This traffic factor contributed 12% of the resolved RM. A major portion, over 90%, of direct vehicle particulate exhaust is carbonaceous compounds, i.e., EC and OC (Amato et al., 2016). In an earlier study on the characterization of $PM_{2.5}$ emitted from diesel vehicles in Asia, EC has been the dominant component, followed by OC and Ca (Kim Oanh et al., 2010) and the EC/OC ratio in the diesel composite source profile measured in Bangkok was 2.4 (Kim Oanh et al., 2010). However, in Hanoi the traffic fleet is dominated by gasoline vehicles, especially motorcycles. In this study the EC/OC mass ratio of the traffic factor was 0.5, which is in the range of the EC/OC ratios measured from motorcycle exhaust (0.24–1) by Panicker et al. (2015). The relatively high proportion of Ni (38%) and V (29%) indicate oil burning, the use of motor oils and/or engine additives (Cohen et al., 2010a). During the COVID-19 restrictions the contribution of the traffic factor was the lowest (Fig. S5).

Factor 2 was a local SIA factor contributing 18% of RM. This factor consists mainly of ammonium, nitrate and chloride (39%, 81% and 66%, respectively) with some sulphate (10%) and trace elements. As the precursor gases of nitrate, NO (42%) and NO_2 (26%), and CO (16%) were found in this factor, we assume this factor consists mainly of SIA formed from the precursor gases emitted by traffic in combination with those from other regional combustion sources, e.g., waste burning. Ammonia, the precursor gas of ammonium, originates not only from agriculture, but also from biomass and waste burning and sewage (See 3.1.2.). The contribution of this factor was lowest in summer (Fig. S5) largely due to the more intensive wet removal and thermodynamic equilibrium of NH_4NO_3 favoring NH_4NO_3 to be in gas phase during warm months.

Factor 3 was a biomass burning factor (BB) with a high contribution of OC (31%), levoglucosan (54%), other sugar anhydrides, and K^+ (41%). This factor contributed 19% of $PM_{2.5}$ which is in line with the earlier calculated contribution of BB, 17% and 21% of RM at the traffic and UGA site (see 3.1.1.). The contribution of this factor was highest during agricultural residue burning (e.g., of rice straw) season. The OC/EC mass ratio of this factor was 29, much higher than the ratio 5.8 found for open field rice straw burning fresh emissions (Kim Oanh et al., 2011). However, the aging of biomass burning aerosol has been found to increase the amount of organic aerosol 1.5- to 6-fold within 3–4 h after emission as secondary organic aerosol are produced by photo-oxidation (Lee et al., 2008). Also, the phase of burning (smoldering vs flaming) affects the OC/EC ratio (Zhang et al., 2013).

Factor 4 was an industry factor with high portions of Zn, Pb, Cd and Mn (76%, 54%, 46% and 38%, respectively). This factor contributed about 9% of RM. Zn concentrations were higher at the traffic site than at the UGA site, indicating a source (e.g., waste combustion) closer to the NCEM. This factor resembled the industrial factors found earlier in Hanoi (Hai and Kim Oanh, 2013; Cohen et al., 2010a), whereas the source has been called a vehicle primary factor in the Hanoi data (Hien et al., 2021) and in Beijing (Srivastava et al., 2021). However, in this study, there were no correlations between typical traffic related gases and this factor (Fig. S5).

Factor 5 was an LRT-SIA factor contributing 25% of RM. The factor consists of ammonium (45%), sulphate (56%) and EC (30%) and some elements, such as V (58%) and Ni (27%), and As, K^+ and Na^+. Ammonium sulphate refers to longer distance transported pollution where SO_2 has oxidized and reacted with ammonia. The combustion of fossil fuels is a typical source of SO_2, but also of As and EC. The V/Ni ratio of this factor was 2, which could refer to heavy oil combustion (Kotchenruther, 2017; Pey et al., 2013, Zhao et al., 2012). This source factor had a higher contribution during winter months when the Northeast Monsoon was more prevalent (Fig. S5).

Factor 6 was a dust factor accounting for 17% of $PM_{2.5}$ RM: The main components of this source were soil minerals Al (46%), Mn (39%), Fe (37%) and Ca (35%). This factor includes also traces of heavy metals and combustion related compounds (i.e., 25% of levoglucosan and 15% of EC). This factor consisted of road dust mixed with traffic related pollutants and PM from construction works and the cement industry. The highest peaks of this source occurred in October–December (Fig. S5). Road dust emissions in Hanoi were found to be significant according to the emission inventory results, i.e., comprising about 20% of the primary $PM_{2.5}$ emissions and by monitoring results in Hanoi (Kim Oanh, 2021).

The comparison between different source apportionment studies is not necessarily straightforward as the naming of the factors is not consistent (Table S2). For example, the ammonium sulphate factor is mostly called an LRT or SIA factor. The factor containing high contribution of Zn and Pb has been assigned as an industry factor (Hai and Kim Oanh, 2013; Cohen et al., 2010a) or a primary vehicle factor (Hien et al., 2021; Srivastava et al., 2021). The ammonium nitrate containing factor found in this study was called a BB factor for a study regarding Beijing (Srivastava et al., 2021), as those compounds are partly emitted from BB. In polluted areas, the recognition of individual sources is challenging, especially during inversion situations with stagnant pollution layers contributed by a variety of sources, and when the data resolution is low (24 h) for separating short-lasting, typically, local emissions. The source apportionment results of this and other studies conducted in Hanoi are presented in Table S2. The results show consistency of major source factors of SIA, industry, BB and traffic. However, in this study, coal combustion was not found as a separate factor, and it was mixed with the other factors e.g., with the LRT and local SIA factors. Coal combustion emits e.g., K^+, Ca^{2+}, Cl^-, heavy metals like As, Cd, Pb and precursor gases of SIA (Table S2 and references herein). Road dust was found to be higher in this study than other studies which may be attributed to our measurement locations and the year-round period of coverage. Hai and Kim Oanh (2013), for example, had the monitoring site located on the rooftop of a 4-storey building (15 m above the ground and 100 m away from a busy road) and sampling was done during December–February when a dizzy weather was prevalently observed, and which subsequently limited dust resuspension due to the wet road surface.

3.4. Analysis of high concentration days

3.4.1. Days with high $PM_{2.5}$ mass

$PM_{2.5}$ concentrations (weighed mass) were high, over 100 μg m^{-3}, on 9 day at the traffic site and on 4 day at the UGA site. To study the worst air pollution situations in detail, four days with high $PM_{2.5}$ concentrations were examined closer using back trajectories and fire maps. On November 11, 2019 there was a high contribution of fires, SIA and As. December 12, 2019 was a BB episode day with a high contribution SIA and oil combustion tracers. January 14, 2020 had a high contribution of Zn, K^+, Ni and SIA. February 21, 2020 was a BB biomass burning day with a lot of OM and SIA.

On November 11, 2019 $PM_{2.5}$ concentrations were high at both measurement sites, 130 μg m^{-3} and 98 μg m^{-3}, at the traffic site and the UGA site respectively, concentrations of SO_2 and NO_2 were increased, and visibility was poor. More than half of the RM was OM, 53 and 43 μg m^{-3}, at the traffic site and the UGA site, respectively (Fig. S6). The concentrations of fire tracers were increased, levoglucosan was 1.6 and 0.9 μg m^{-3} and potassium 1.7 and 1.4 μg m^{-3}, at the traffic and UGA site, respectively, and 15 fire counts were detected in the Red River Delta Domain. In addition, the concentrations of As and SIA were high, and sulphate peaked up to 16 μg m^{-3} likely indicating coal combustion. Backwards trajectories showed air masses arriving from the north-east carrying pollutants from Northern Vietnam and South China. In addition, the nocturnal boundary layer height was low (42 m), and wind speed was low (1.4 m/s, daily average) which indicates stagnant atmospheric conditions and supports the accumulation of local pollutants.

In December there was an intensive biomass burning episode in the Red River Delta domain. On 4 December $PM_{2.5}$, levoglucosan and K^+

concentrations were quite moderate despite of the high number of fires (224 fire counts), but the fires were clearly seen in the chemical composition of samples collected on 10, 12 and December 14, 2019. At the UGA site, the maximum concentrations of fire tracers (levoglucosan of 2.1 μg m^{-3} and K^+ of 2.0 μg m^{-3}), were measured on 10 December (228 fire counts) and at the traffic site two days later. **On December 12, 2019** $PM_{2.5}$ concentrations were 174 μg m^{-3} at the traffic and 166 μg m^{-3} at the UGA site and over 60% of RM was OM at both sites (Fig. 7). Levoglucosan was 1.7 μg m^{-3} and 1.5 μg m^{-3} at the traffic and the UGA site, respectively. SIA concentrations were elevated and nitrate concentrations of 10.4 and 12.6 μg m^{-3} peaked to be higher than sulphate of 10.0 and 11.2 μg m^{-3} at the traffic and UGA site, respectively. Of the trace elements, especially arsenic was high at both sites and at the UGA site also Cr, Ni and V peaked indicating heavy oil combustion or an industrial source. In addition, Zn, Cd and Cl^- peaked at the traffic site (see section 3.1.4.). The aerosol optical depth was about 1.0 indicating a very high number of airborne particles in Hanoi atmosphere. On the fire maps of those days, there were 190 fire spots in the Red River Delta, 1556 in the Northern Vietnam Domain and 2983 fire counts in the Domain of Norther Vietnam & South China. Air masses were circulating over Northeastern Vietnam before arriving at Hanoi from the south. 12 December was the coldest of all the measurement days with a daily average temperature of 13 °C. On these episode days atmospheric mixing was limited as nocturnal BLH (<50 m), and the daily average wind speed were low (<1 m/s).

On January 14, 2020, $PM_{2.5}$ concentrations were very high, 177 and 188 μg m^{-3} at the traffic and UGA site, respectively, and there was a high contribution of all measured compounds, especially heavy metals, and a minor effect of biomass burning (Fig. S7). There were no fires detected in the Red River Delta Domain, but 136 fires in Northern Vietnam, and 661 in Northern Vietnam & South China. Zn and Cd concentrations were higher at the UGA site (6 μg m^{-3} and 9.5 ng m^{-3}) than at the traffic site (5 μg m^{-3} and 5.7 ng m^{-3}) and similarly Cl^-, SO_4^{2-}, and NO_3^- peaked at the UGA site, possibly indicating emissions from coal combustion. In addition, at the traffic site EC and Ni were peaking high. The backwards trajectory of the day showed air masses entering the region from the south passing the Thanh Hoa Province after having a long marine pathway through the Gulf of Tonkin.

On February 21, 2020 $PM_{2.5}$ concentrations were very high, 167 and 183 μg m^{-3} at the NCEM and the Hanoi EPA, respectively. Concentrations of fire tracers, K^+ and levoglucosan were higher at the UGA site (1.0 and 1.0 μg m^{-3}) than at the traffic site (0.77 and 0.83 μg m^{-3}) and OC was peaking, but EC was low indicating a contribution from biomass burning and the presence of aged organic aerosol. The contribution of nitrate in $PM_{2.5}$ mass was higher than sulphate and the concentrations of trace elements were low, indicating that there was less influence of industrial sources than usually. At the traffic site, 50% of the RM was OM and 40% was SIA, and at the UGA site, 48% was OM and 47% was SIA, respectively. There was just one fire hot spot in the Red River Delta domain, but 311 and 1060 fire counts in Northern Vietnam and in the Northern Vietnam & South Chine domain, respectively. Most of the fire spots were in east of Hanoi and air masses were coming from the east passing Hainan Island and the Gulf of Tokin, possibly carrying organic aerosol from the fire area. The average wind speed at Noi Bai in Hanoi was 2.7 m/s. The BLHs were not so low (184 m at 1 a.m., 994 m at 13 p.m.) (Fig. S8).

3.4.2. *Days with high Zn concentrations*

Among the measurement days, there were ten days with Zn concentrations above 4 μg m^{-3} at the traffic site, but only 2 day at the UGA

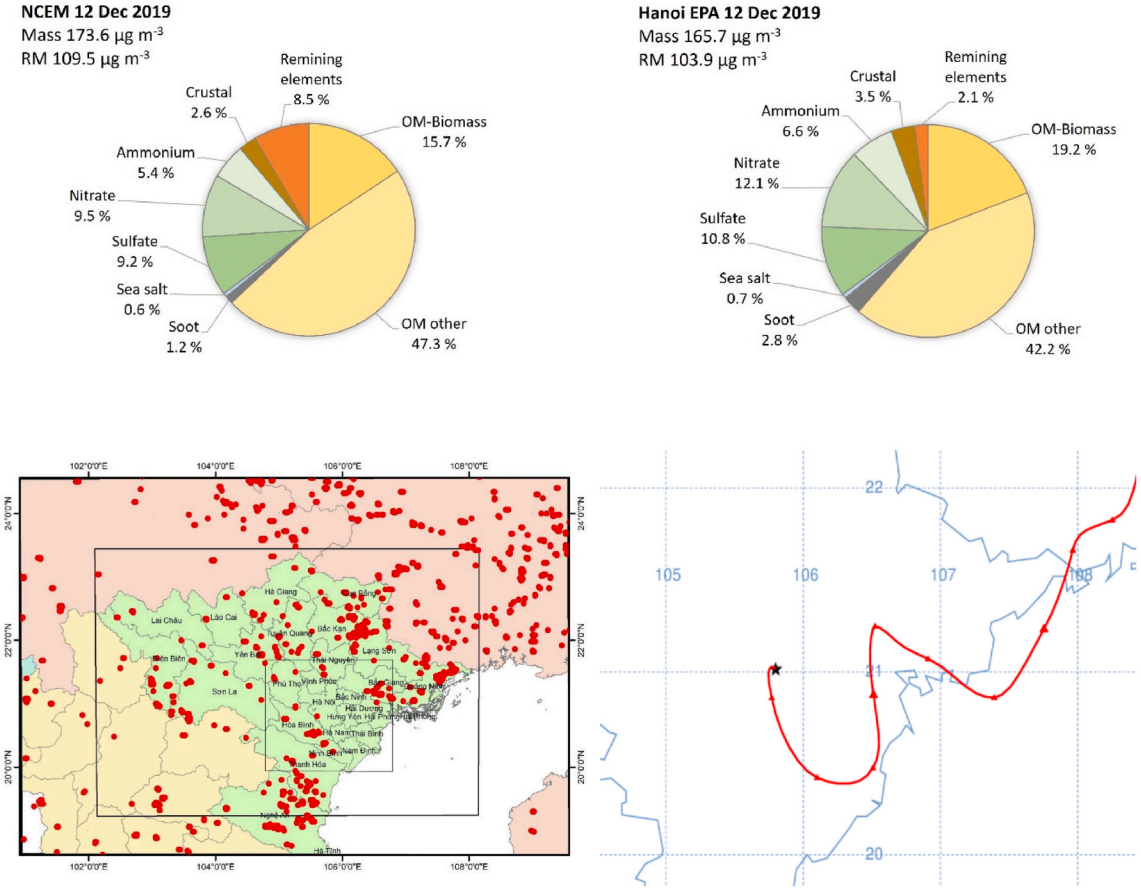

Fig. 7. Chemical composition of the $PM_{2.5}$ reconstructed mass on December 12, 2019 at the traffic site (NCEM) and the UGA site (Hanoi EPA) (pie charts). Fire map: active fires marked with red spots (on the left) and HYSPLIT 72 h backward trajectory at 7 a.m. (at 00:00 UTC) showing the transport of air masses (on the right).

site (Fig. 5). Of those days, the five highest Zn concentrations (>5 μg m^{-3}) that were measured at the traffic site on October 10, 2019 (17.0 μg m^{-3}), December 23, 2019 (15.8 μg m^{-3}), September 11, 2019 (9.6 μg m^{-3}), November 21, 2019 (8.1 μg m^{-3}) and January 14, 2020 (5.3 μg m^{-3}), were not included in the PMF analysis. On all the high Zn concentration days, the nocturnal boundary layer height was low (below 100 m at 1:00), indicating inversion situations and limited atmospheric mixing. On the days with high Zn concentrations (>4 μg m^{-3}), Cl^-, Cd, and EC also peaked. On four out of ten high Zn concentration days at the traffic site, there was Cl^- excess in the samples, when calculating the molar fractions of inorganic secondary ions (NH_4^+, NO_3^-, SO_4^{2-} and Cl^-), possibly indicating the presence of water soluble $ZnCl_2$ used, e.g., in the manufacturing of fabrics and in batteries. As all the Zn peaks were much higher at the traffic site, it showed that a strong local Zn source, e.g., open backyard solid waste burning was closer to the traffic site (NCEM) than to the UGA site (Hanoi EPA). Besides, the traffic site is in the eastern side of the Hanoi city, not far from the industrial area. Also, the Bac Ninh area with scrap metal recycling and forging and copper casting villages that is east of the traffic site could be a possible source of regional pollution transport. Compared to previous studies in Hanoi in 2001–2008 (Cohen et al., 2010a) and during Nov 2015–June 2016 (Hien et al., 2021), the Zn and Cl^- concentrations in our study were remarkably higher, especially at the traffic site. Further studies are required to separate the contributions of different sources such as industrial sources, coal power plants, and coal briquette and waste burning.

Three days with very high contributions of zinc at the traffic site, October 10, 2019, November 21, 2019, and January 14, 2020, were studied using back trajectories and fire maps (see Fig S9, S10 and S7). On **October 10, 2019** the $PM_{2.5}$ concentration at the traffic site, 91 μg m^{-3}, was twice as high as at the UGA site, 45 μg m^{-3}. At the traffic site, the EC concentration (8.5 μg m^{-3}) was double compared to the UGA site (4 μg m^{-3}). In addition, heavy metal concentrations were unexceptionally high at the traffic site (Zn 17 μg m^{-3}, Pb 0.5 μg m^{-3} and Cd 12 ng m^{-3}), as was the Cl^- concentration (5 μg m^{-3}). According to the trajectories, air masses came from the south and south-east (Fig. S9).

On November 21, 2019, the $PM_{2.5}$ concentration was higher at the traffic site (82 μg m^{-3}) than at the UGA site (68 μg m^{-3}). At the traffic site K^+ and levoglucosan concentrations were elevated, although there was just one fire spot detected in the Red River Delta. The concentrations of Zn (8 μg m^{-3}), Cd (17 ng m^{-3}), Mn (236 ng m^{-3}), and Cl^-.

(3 μg m^{-3}) peaked. Air masses from the north-east were arriving at Hanoi from the east (Fig. S10). Atmospheric dispersion was limited by the low wind speed (<1 m/s in Hanoi city) and low nocturnal BLH (39 m).

4. Conclusions

This study presents a one-year time series of $PM_{2.5}$ mass and chemical composition measured in Hanoi at a traffic site (NCEM station) and an urban general area (UGA, Hanoi EPA station). The $PM_{2.5}$ annual average concentrations measured at the traffic and the UGA site, 49 and 46 μg m^{-3}, respectively, highly exceeded the annual AQ standard for $PM_{2.5}$ in Vietnam (25 μg m^{-3}, (QCVN 05, 2013)). The national daily standard (50 μg m^{-3}) was also repeatedly exceeded, especially with a high frequency in winter on the days with stagnant meteorological conditions. The annual average of measured $PM_{2.5}$ concentrations in Hanoi is about ten times higher than the 2021 WHO AQG for $PM_{2.5}$ (5 μg m^{-3}), thus indicating a severe health concern for the population of Hanoi.

In the source apportionment of the $PM_{2.5}$ resolved mass, six source factors were found. Two of them were for secondary inorganic aerosol: one was long-range transported (25%) with high sulphate concentration and the other one a more locally originated (18%) with high contribution of nitrate. The other four factors were biomass burning (19%), dust (17%), traffic (12%) and industry (9%). About half of the resolved aerosol mass was organic matter, and one third was secondary inorganic aerosol. On average, 10% of the resolved mass was soot at the traffic site, and twice as much as at the UGA site. However, during the COVID-19 traffic restrictions in April, the EC concentrations at the traffic site were halved.

The toxic trace elements As, Cd, Pb, and Ni measured in $PM_{2.5}$ did not exceed the WHO air quality guidelines for PM_{10}-based annual averages. However, there were days with high concentrations of these elements and Zn as well as Cl^-. Arsenic especially peaked in winter, likely originating from coal combustion. Zn concentrations were occasionally very high at the traffic site, often simultaneously with Cl^-, Pb and Cd, indicating a strong pollution source, possibly waste combustion, close to the traffic site. Emissions from waste burning, industrial sources, and traffic contain heavy metals that increase the toxicity of the particles and cause adverse health effects on the population.

These monitoring results have been used for the verification of the GAINS model results that show consistency in the $PM_{2.5}$ levels and compositions at both sites. The findings of this study are an important input to the development of effective and cost-effective measures to reduce air pollution in Hanoi. There is an urgent need for further, preferably continuous, measurements of the chemical composition of $PM_{2.5}$ to study the effects of interventions in improving air quality.

CRediT authorship contribution statement

Ulla Makkonen: Conceptualization, starting measurements, quality control of, Formal analysis, data handling, Writing – original draft, Writing – review & editing. **Mika Vestenius:** starting measurements, Investigation, Writing – review & editing. **L.N. Huy:** fire maps, trajectories, Writing – review & editing. **N.T.N. Anh:** facilities and leading the project at NCEM, Writing – review & editing. **P.T.V. Linh:** measurements at NCEM, Writing – review & editing. **P.T. Thuy:** gravimetric analysis at NCEM, Writing – review & editing. **H.T.M. Phuong:** filter sampling at NCEM, Writing – review & editing. **Huyen Nguyen:** facilities and leading the project at Hanoi EPA, Writing – review & editing. **L. T. Thuy:** filter sampling at Hanoi EPA, Writing – review & editing. **Minna Aurela:** EC/OC analysis, writing, Writing – review & editing. **Heidi Hellén:** facilities, leading the FMI research group, Writing – review & editing, supported and supervised the research and commented on the manuscript. **Katja Loven:** the project leader, financing leader, Writing – review & editing. **Rostislav Kouznetsov:** boundary layer heights, supporting in meteorological questions, Writing – review & editing. **Katriina Kyllönen:** quality control issues, Writing – review & editing. **Kimmo Teinilä:** sugar anhydride measurements, Writing – review & editing, writing. **N.T. Kim Oanh:** writing, Writing – review & editing, supported and, Supervision, the research .

Declaration of competing interest

The authors declare that they have no known competing financial interests or personal relationships that could have appeared to influence the work reported in this paper.

Data availability

Data will be made available on request.

Acknowledgement

This work has been supported by the World Bank (Group contract 7191921).

We thank all our colleagues from NCEM, Hanoi EPA, FMI and Finnish Environment Institute colleagues for their valuable support and help in this study.

Appendix A. Supplementary data

Supplementary data to this article can be found online at https://doi.org/10.1016/j.atmosenv.2023.119650.

References

Achilleos, S., Kioumourtzoglou, M.A., Wu, C.D., Schwartz, J.D., Koutrakis, P., Papatheodorou, S.I., 2017. Acute effects of fine particulate matter constituents on mortality: a systematic review and meta-regression analysis. Environ. Int. 109, 89–100. https://doi.org/10.1016/j.envint.2017.09.010.

Almeida, S.M., Manousakas, M., Diapouli, E., Kertesz, Z., Samek, L., Hristova, E., Šega, K., Padilla Alvarez, R., Belis, C.A., Eleftheriadis, K., 2020. Ambient particulate matter source apportionment using receptor modelling in European and Central Asia urban areas. Environ. Pollut. 266 (3), 115199 https://doi.org/10.1016/j.envpol.2020.115199. ISSN 0269-7491.

Amato, F., Alastuey, A., Karanasiou, A., Lucarelli, F., Nava, S., Calzolai, G., Severi, M., Becagli, S., Gianelle, V.L., Colombi, C., Alves, C., Custódio, D., Nunes, T., Cerqueira, M., Pio, C., Eleftheriadis, K., Diapouli, E., Reche, C., Minguillón, M.C., Manousakas, M.-I., Maggos, T., Vratolis, S., Harrison, R.M., Querol, X., 2016. AIRUSE-LIFE+: a harmonized PM speciation and source apportionment in five southern European cities. Atmos. Chem. Phys. 16, 3289–3309. https://doi.org/10.5194/acp-16-3289-2016.

Belis, C.A., Karagulian, F., Larsen, B.R., Hopke, P.K., 2013. Critical review and meta-analysis of ambient particulate matter source apportionment using receptor models in Europe. Atmos. Environ. 69, 94–108. https://doi.org/10.1016/j.atmosenv.2012.11.009. ISSN 1352-2310.

Cavalli, F., Viana, M., Yttri, K.E., Genberg, J., Putaud, J.-P., 2010. Toward a standardised thermal-optical protocol for measuring atmospheric organic and elemental carbon: the EUSAAR protocol. Atmos. Meas. Tech. 3, 79–89. https://doi.org/10.5194/amt-3-79-2010.

Cheng, Y., Engling, G., He, K.-B., Duan, F.-K., Ma, Y.-L., Du, Z.-Y., Liu, J.-M., Zheng, M., Weber, R.J., 2013. Biomass burning contribution to Beijing aerosol. Atmos. Chem. Phys. 13, 7765–7781. https://doi.org/10.5194/acp-13-7765-2013.

Chow, J.C., Lowenthal, D.H., Chen, L.W., Wang, X., Watson, J.G., 2015. Mass reconstruction methods for PM2.5: a review. Air Qual Atmos Health 8, 243–263. https://doi.org/10.1007/s11869-015-0338-3.

Cohen, D.D., Crawford, J., Stelcer, E., Bac, V.T., 2010a. Characterization and source apportionment of fine particulate sources at Hanoi from 2001 to 2008. Atmos. Environ. 44, 320–328. https://doi.org/10.1016/j.atmosenv.2009.10.037.

Cohen, D.D., Crawford, J., Stelcer, E., Bac, V.T., 2010b. Long range transport of fine particle windblown soils and coal fired power station emissions into Hanoi between 2001 to 2008. Atmos. Environ. 44, 3761–3769. https://doi.org/10.1016/j.atmosenv.2010.06.047.

Crippa, M., Canonaco, F., Lanz, V., Aijala, M., Allan, J., Carbone, S., Capes, G., Ceburnis, D., Dall'Osto, M., Day, D., DeCarlo, P., Ehn, M., Eriksson, A., Freney, E., Hildebrandt Ruiz, L., Hillamo, R., Jimenez, J., Junninen, H., Kiendler-Scharr, A., Kortelainen, A., Kulmala, M., Laaksonen, A., Mensah, A., Mohr, C., Nemitz, E., O'Dowd, C., Ovadnevaite, J., Pandis, S., Petaja, T., Poulain, L., Saarikoski, S., Sellegri, K., Swietlicki, E., Tiitta, P., Worsnop, D., Baltensperger, U., Prevot, A., 2014. Organic aerosol components derived from 25 AMS data sets across Europe using a consistent ME-2 based source apportionment approach. Atmos. Chem. Phys. 14, 6159–6176. https://doi.org/10.5194/acp-14-6159-2014.

Diapouli, E., Popovicheva, O., Kistler, M., Vratolis, S., Persiantseva, N., Timofeev, M., Kasper-Giebl, A., Eleftheriadis, K., 2014. Physicochemical characterization of aged biomass burning aerosol after long-range transport to Greece from large scale wildfires in Russia and surrounding regions, Summer 2010. Atmos. Environ. 96, 393–404. https://doi.org/10.1016/j.atmosenv.2014.07.055.

Ding, A.J., Huang, X., Nie, W., Sun, J.N., Kerminen, V.-M., Petäjä, T., Su, H., Cheng, Y.F., Yang, X.-Q., Wang, M.H., Chi, X.G., Wang, J.P., Virkkula, A., Guo, W.D., Yuan, J., Wang, S.Y., Zhang, R.J., Wu, Y.F., Song, Y., Zhu, T., Zilitinkevich, S., Kulmala, M., Fu, C.B., 2016. Enhanced haze pollution by black carbon in megacities in China, Geophys. Res. Lett. 43 https://doi.org/10.1002/2016GL067745.

14902 EN, 2005. Ambient Air Quality. Standard Method for the Measurement of Pb, Cd, as and Ni in the PM10 Fraction of Suspended Particulate Matter, AC:2006.

EN, 2014. Ambient Air. Standard Gravimetric Measurement Method for the Determination of PM_{10} or $PM_{2.5}$ Mass Concentration of Suspended Particulate Matter, 12341.

EN, 2017a. Ambient Air - Measurement of Elemental Carbon (EC) and Organic Carbon (OC) Collected on Filters, 16909.

EN, 2017b. Ambient Air - Standard Method for Measurement of NO_3^-, SO_4^{2-}, Cl^-, NH_4^+, Na^+, K^+, Mg^{2+}, Ca^{2+} in $PM_{2.5}$ as Deposited on Filters, 16913.

107 EU Directive, 2004. EC of the European Parliament and of the Council of 15 December 2004 relating to arsenic, cadmium, mercury, nickel and polycyclic aromatic hydrocarbons in ambient air. http://data.europa.eu/eli/dir/2004/107/2015-09-18.

GSO, 2020. General Statistics Office of Viet Nam: General Statistic Office of Vietnam. Statistical Yearbook of Vietnam 2019. Statistical Publishing House, Hanoi. https://www.gso.gov.vn.

Hai, C.D., Kim Oanh, N.T., 2013. Effects of local, regional meteorology and emission sources on mass and compositions of particulate matter in Hanoi. Atmos. Environ. 78, 105–112. https://doi.org/10.1016/j.atmosenv.2012.05.006.

He, G., Pan, Y., Tanaka, T., 2020. The short-term impacts of COVID-19 lockdown on urban air pollution in China. Nat. Sustain. 3, 1005–1011. https://doi.org/10.1038/s41893-020-0581-y.

HEI, 2020. Health Effects Institute. State of Global Air/2020. A special report on global exposure to air pollution and its impacts. Available at: https://www.stateofglobalair.org/.

Hien, P.D., Bac, V.T., Tham, H.C., Nhan, D.D., Vinh, L.D., 2002. Influence of meteorological conditions on PM2.5 and PM2.5−10 concentrations during the monsoon season in Hanoi, Vietnam. Atmos. Environ. 36, 3473–3484. https://doi.org/10.1016/S1352-2310(02)00295-9.

Hien, P.D., Loc, P.D., Dao, N.V., 2011. Air pollution episodes associated with East Asian winter monsoons. Sci. Total Environ. 409 (23), 5063–5068. https://doi.org/10.1016/j.scitotenv.2011.08.049.

Hien, P.D., Bac, V.T., Thinh, N.T.H., Anh, H.L., Thang, D.D., Nghia, N.T., 2021. A comparison study of chemical compositions and sources of $PM_{1.0}$ and $PM_{2.5}$ in Hanoi. Aerosol Air Qual. Res. 21, 210056 https://doi.org/10.4209/aaqr.210056.

Holme, J.A., Brinchmann, B.C., Refsnes, M., Låg, M., Øvrevik, J., 2019. Potential role of polycyclic aromatic hydrocarbons as mediators of cardiovascular effects from combustion particles. Environ. Health 18, 74. https://doi.org/10.1186/s12940-019-0514-2.

Hopke, P.K., 2016. Review of receptor modeling methods for source apportionment. J. Air Waste Manag. Assoc. 66, 237–259. https://doi.org/10.1080/10962247.2016.1140693.

Hopke, P.K., Cohen, D.D., Begum, B.A., Biswas, S.K., Ni, B., Pandit, G.G., Santoso, M., Chung, Y.-S., Rahman, S.A., Hamzah, M.S., Davy, P., Markwitz, A., Waheed, S., Siddique, N., Santos, F.L., Pabroa, P.C.B., Seneviratne, M.C.S., Wimolwattanapun, W., Bunprapob, S., Vuong, T.B., Markowicz, A., 2008. Urban air quality in the Asian region. Sci. Total Environ. 404 (1), 103–112. https://doi.org/10.1016/j.scitotenv.2008.05.039.

Hopke, P.K., Dai, Q., Li, L., Feng, Y., 2020. Global review of recent source apportionments for airborne particulate matter. Sci. Total Environ. 740, 140091 https://doi.org/10.1016/J.Scitotenv.2020.140091.

Huang, Y., Jin, B., Zhong, Z., Xiao, R., Tang, Z., Ren, H., 2004. Trace elements (Mn, Cr, Pb, Se, Zn, Cd and Hg) in emissions from a pulverized coal boiler. Fuel Process. Technol. 86 (1), 23–32. https://doi.org/10.1016/j.fuproc.2003.10.022.

Huy, L.N., Kim Oanh, N.T., 2017. Assessment of national emissions of air pollutants and climate forcers from thermal power plants and industrial activities in Vietnam. Atmos. Pollut. Res. 8 (3), 503–513. https://doi.org/10.1016/j.apr.2016.12.007.

Huy, L.N., Kim Oanh, N.T., Phuc, N.H., Nhung, C.P., 2021. Survey-based inventory for atmospheric emissions from residential combustion in Vietnam. Environ. Sci. Pollut. Res. 28, 10678–10695. https://doi.org/10.1007/s11356-020-11067-6.

India, A.Q.S., 2009. National ambient air quality standards, as of 2009. https://www.transportpolicy.net/standard/india-air-quality-standards/. (Accessed 2 December 2021).

Jalava, P.I., Salonen, R.O., Pennanen, A.S., Sillanpää, M., Hälinen, A.I., Happo, M.S., Hillamo, R., Brunekreef, B., Katsouyanni, K., Sunyer, J., Hirvonen, M.-R., 2007. Heterogeneities in inflammatory and cytotoxic responses of RAW 264.7 macrophage cell line to urban air coarse, fine, ultrafine particles from six European sampling campaigns. Inhal. Toxicol. 19, 213–225. https://doi.org/10.1080/08958370601067863.

Kim Oanh, N.T., 2021. Rice straw open burning: emissions, effects and multiple benefits of non-burning alternatives. Vietnam Journal of Science Technology and Engineering 63 (4), 79–85. https://doi.org/10.31276/VJSTE.63(4).79-85. https://vietnamscience.vjst.vn/index.php/VJSTE/announcement/abstract159.

Kim Oanh, N.T., Upadhyay, N., Zhuang, Y.H., Hao, Z.P., Murthy, D.V.S., Lestari, P., Villarine, J.T., Chengchua, K., Co, H.X., Dung, N.T., Lindgren, E.S., 2006. Particulate air pollution in six Asian cities: spatial and temporal distributions, and associated sources. Atmos. Environ. 40, 3367–3380. https://doi.org/10.1016/j.atmosenv.2006.01.050.

Kim Oanh, N.T., Thiansathit, W., Bond, T.C., Subramanian, R., Ekbordin, W., Ittipol, P., 2010. Compositional characterization of PM2.5 emitted from in-use diesel vehicles in Asia. Atmos. Environ. 44, 15–22. https://doi.org/10.1016/j.atmosenv.2009.10.005.

Kim Oanh, N.T., Thuy, L.B., Tipayarom, D., Manadhar, D.R., Pongkiatkul, P., Simpson, C. D., Liu, S.L.J., 2011. Characterization of particulate matter emission from open burning of rice straw. Atmos. Environ. 45, 493–502. https://doi.org/10.1016/j.atmosenv.2010.09.023.

Kotchenruther, R.A., 2017. The effects of marine vessel fuel sulfur regulations on ambient $PM_{2.5}$ at coastal and near coastal monitoring sites in the. U.S. Atmospheric Environment 151, 52–61. https://doi.org/10.1016/j.atmosenv.2016.12.012.

Kyllönen, K., Vestenius, M., Anttila, P., Makkonen, U., Aurela, M., Wängberg, I., Nerentorp Mastromonaco, M., Hakola, H., 2020. Trends and source apportionment of atmospheric heavy metals at a subarctic site during 1996–2018. Atmos. Environ. 236, 117644 https://doi.org/10.1016/j.atmosenv.2020.117644.

Le, H.A., Phuong, D.M., Linh, L.T., 2020. Emission inventories of rice straw open burning in the Red River Delta of Vietnam: evaluation of the potential of satellite data. Environ. Pollut. 260, 113972 https://doi.org/10.1016/j.envpol.2020.113972.

Lee, S.C., Cheng, Y., Ho, K.F., Cao, J.J., Louie, P.K.-K., Chow, J.C., Watson, J.G., 2006. PM1.0 and PM2.5 characteristics in the roadside environment of Hong Kong. Aerosol. Sci. Technol. 40, 157–165. https://doi.org/10.1080/02786820500494544.

Lee, S., Kim, H.K., Yan, B., Cobb, C.E., Hennigan, C., Nichols, S., Chamber, M., Edgerton, E.S., Jansen, J.J., Hu, Y.T., Zheng, M., Weber, R.J., Russell, A.G., 2008. Diagnosis of aged, prescribed plumes impacting an urban area. Environ. Sci. Tecnol. 42, 1438–1444. https://doi.org/10.1021/es7023059.

Li, Y., Fu, T.-M., Yu, J.Z., Feng, X., Zhang, L., Chen, J., Suresh Kumar Reddy, B., Kawamura, K., Fu, P., Yang, X., Zhu, L., Zeng, Z., 2021. Impacts of chemical

degradation on the global budget of atmospheric levoglucosan and its use as a biomass burning tracer. Environ. Sci. Technol. 55, 5525–5536. https://doi.org/10.1021/acs.est.0c07313.

Lu, X., Lin, C., Li, W., Chen, Y., Huang, Y., Fung, J.C.H., Lau, A.K.H., 2019. Analysis of the adverse health effects of PM2.5 from 2001 to 2017 in China and the role of urbanization in aggravating the health burden. Sci. Total Environ. 652, 683–695. https://doi.org/10.1016/j.scitotenv.2018.10.140.

Luong, L.T.M., Dang, T.N., Thanh Huong, N.T., Phung, D., Tran, L.K., Van Dung, D., Thai, P.K., 2020. Particulate air pollution in Ho Chi Minh city and risk of hospital admission for acute lower respiratory infection (ALRI) among young children. Environ. Pollut. 257, 113424 https://doi.org/10.1016/j.envpol.2019.113424.

Ly, B.-T., Kajii, Y., Nguyen, T.-Y.-L., Shoji, K., Van, D.-A., Do, T.-N.-N., Sakamoto, Y., 2020. Characteristics of roadside volatile organic compounds in an urban area dominated by gasoline vehicles, a case study in Hanoi. Chemosphere 254, 126749. https://doi.org/10.1016/j.chemosphere.2020.126749.

Ly, B.-T., Matsumi, Y., Vu, T.V., Sekiguchi, K., Nguyen, T.-T., Pham, C.-T., Nghiem, T.-D., Ngo, I.-H., Kurotsuchi, Y., Nguyen, T.-H., Nakayama, T., 2021. The effects of meteorological conditions and long-range transport on PM2.5 levels in Hanoi revealed from multi-site measurement using compact sensors and machine learning approach. J. Aerosol Sci. 152, 105716 https://doi.org/10.1016/j.jaerosci.2020.105716.

Makkonen, U., Hellén, H., Anttila, P., Ferm, M., 2010. Size distribution and chemical composition of airborne particles in south-eastern Finland during different seasons and wildfire episodes in 2006. Sci. Total Environ. 408, 644–651. https://doi.org/10.1016/j.scitotenv.2009.10.050.

Ngoc, B.A.P., Delbarre, H., Deboudt, K., Dieudonné, E., Tran, D.N., Thanh, S.L., Pelon, J., Ravetta, F., 2021. Key factors explaining severe air pollution episodes in Hanoi during 2019 winter season. Atmos. Pollut. Res. 12, 6. https://doi.org/10.1016/j.apr.2021.101068.

Ngu, N.D., Hieu, N.T., 2004. Climate and Climate Resources of Vietnam (Khi Hau Va Tai Nguyen Khi Hau, Vietnam). IHA. Agriculture Publisher, Hanoi, Vietnam.

Nguyen, T.P.M., Bui, T.H., Nguyen, M.K., Nguyen, T.H., Vu, V.T., Pham, H.L., 2021. Impact of COVID-19 partial lockdown on PM2.5, SO2, NO2, O3, and trace elements in PM2.5 in Hanoi. Vietnam. Environ. Sci. Pollut. Res. 1–11. https://doi.org/10.1007/s11356-021-13792-y.

Nhung, N.T.T., Schindler, C., Dien, T.M., Probst-Hensch, N., Perez, L., Künzli, N., 2018. Acute effects of ambient air pollution on lower respiratory infections in Hanoi children: an eight-year time series study. Environ. Int. 110, 139–148. https://doi.org/10.1016/j.envint.2017.10.024.

US EPA 2014 Norris, G., Duvall, R., Brown, S., Bai, S., 2014. EPA positive matrix factorization (PMF) 5.0 fundamentals and user guide, EPA/600/R-14/108. https://www.epa.gov/sites/default/files/2015-02/documents/pmf_5.0_user_guide.pdf. (Accessed 11 March 2022).

Nowak, J.B., Neuman, J.A., Bahreini, R., Brock, C.A., Middlebrook, A.M., Wollny, A.G., Holloway, J.S., Peischl, J., Ryerson, T.B., Fehsenfeld, F.C., 2010. Airborne observations of ammonia and ammonium nitrate formation over Houston, Texas. J. Geophys. Res. 115, D22304 https://doi.org/10.1029/2010JD014195.

Paatero, P., 1997. Least squares formulation of robust non-negative factor analysis. Chemometr. Intell. Lab. Syst. 37, 23–35. https://doi.org/10.1016/S0169-7439(96)00044-5.

Paatero, P., Tapper, U., 1994. Positive matrix factorization: a non-negative factor model with optimal utilization of error estimates of data values. Environmetrics 5, 111–126. https://doi.org/10.1002/env.3170050203.

Pacyna, J.M., Pacyna, E.G., 2001. An assessment of global and regional emissions of trace metals to the atmosphere from anthropogenic sources worldwide. Environ. Rev. 9, 269–298. https://doi.org/10.1139/a01-012.

Pacyna, J.M., Pacyna, E.G., Aas, W., 2009. Changes of emissions and atmospheric deposition of mercury, lead, and cadmium. Atmos. Environ. 43 (1), 117–127. https://doi.org/10.1016/j.atmosenv.2008.09.066.

Panicker, A.S., Ali, K., Beig, G., Yadav, S., 2015. Characterization of particulate matter and carbonaceous aerosol over two urban environments in northern India. Aerosol Air Qual. Res. 15, 2584–2595. https://doi.org/10.4209/aaqr.2015.04.0253.

Pant, P., Shukla, A., Kohl, S.D., Chow, J.C., Watson, J.G., Harrison, R.M., 2015. Characterization of ambient PM2.5 at a pollution hotspot in New Delhi, India and inference of sources. Atmos. Environ. 109, 178–189. https://doi.org/10.1016/j.atmosenv.2015.02.074.

Pathak, R.K., Yao, X., Alexis, K.H., Lau, A.K.H., Chan, C.K., 2003. Acidity and concentrations of ionic species of PM2.5 in Hong Kong. Atmos. Environ. 37, 1113–1124. https://doi.org/10.1016/S1352-2310(02)00958-5.

Petäjä, T., Järvi, L., Kerminen, V.-M., Ding, A.J., Sun, J.N., Nie, W., Kujansuu, J., Virkkula, A., Yang, X.-Q., Fu, C.B., Zilitinkevich, S., Kulmala, M., 2016. Enhanced air pollution via aerosol-boundary layer feedback in China. Sci. Rep. 6, 18998 https://doi.org/10.1038/srep18998.

Pey, J., Perez, N., Cortés, J., Alastuey, A., Querol, X., 2013. Chemical fingerprint and impact of shipping emissions over a western Mediterranean metropolis: primary and aged contributions. Sci. Total Environ. 497–507. https://doi.org/10.1016/j.scitotenv.2013.06.061, 463-464.

Phuc, N.H., Oanh, N.T.K., 2018. Determining factors for levels of volatile organic compounds measured in different microenvironments of a heavy traffic urban area. Sci. Total Environ. 627, 290–303. https://doi.org/10.1016/j.scitotenv.2018.01.216.

Phuc, N.H., Oanh, N.T.K., 2021. Large spatio-temporal variations of size-resolved particulate matter and volatile organic compounds in urban area with heavy traffic. Environ. Sci. Pollut. Res. 29 (15), 21491–21507. https://doi.org/10.1007/s11356-021-16921-9.

Phung, D., Hien, T.T., Linh, H.N., Luong, L.M.T., Morawska, L., Chu, C., Binh, N.D., Thai, P.K., 2016. Air pollution and risk of respiratory and cardiovascular hospitalizations in the most populous city in Vietnam. Sci. Total Environ. 557, 322–330. https://doi.org/10.1016/j.scitotenv.2016.03.070.

Ramanathan, V., Carmichael, G., 2008. Global and regional climate changes due to black carbon. Nat. Geosci. 1, 221–227. https://doi.org/10.1038/ngeo156.

Rolph, G., Stein, A., Stunder, B., 2017. Real-time environmental applications and display sYstem: ready. Environ. Model. Software 95, 210–228. https://doi.org/10.1016/j.envsoft.2017.06.025.

Roy, S., Lam, Y.F., Hung, N.T., Chan, J.C.L., Fu, J.S., 2021. Development of 2015 Vietnam emission inventory for power generation units. Atmos. Environ. 247, 118042 https://doi.org/10.1016/j.atmosenv.2020.118042.

Saarnio, K., Teinilä, K., Saarikoski, S., Carbone, S., Gilardoni, S., Timonen, H., Aurela, M., Hillamo, R., 2013. Online determination of levoglucosan in ambient aerosols with particle-into-liquid sampler – high-performance anion-exchange chromatography – mass spectrometry (PILS–HPAEC–MS). Atmos. Meas. Tech. 6, 2839–2849. https://doi.org/10.1080/10962247.2016.1140693.

Shiel, A.E., Weis, D., Orians, K.J., 2010. Evaluation of zinc, cadmium and lead isotope fractionation during smelting and refining. Sci. Total Environ. 408 (11), 2357–2368. https://doi.org/10.1016/j.scitotenv.2010.02.016.

Simoneit, B.R.T., 2002. Biomass burning — a review of organic tracers for smoke from incomplete combustion. Appl. Geochem. 17, 129–162. https://doi.org/10.1016/S0883-2927(01)00061-0.

Simoneit, B.R.T., Schauer, J.J., Nolte, C.G., Oros, D.R., Elias, V.O., Fraser, M.P., Rogge, W.F., Cass, G.R., 1999. Levoglucosan, a tracer for cellulose in biomass burning and atmospheric particles. Atmos. Environ. 33, 173–182. https://doi.org/10.1016/S1352-2310(98)00145-9.

Squizzato, S., Masiol, M., Emami, F., Chalupa, D.C., Utell, M.J., Rich, D.Q., Hopke, P.K., 2019. Long-Term changes of source apportioned particle number concentrations in a metropolitan area of the northeastern United States. Atmosphere 10, 27. https://doi.org/10.3390/atmos10010027.

Srivastava, D., Xu, J., Vu, T.V., Liu, D., Li, L., Fu, P., Hou, S., Shi, Z., Harrison, R.M., 2021. Insight into PM2.5 sources by applying positive matrix factorization (PMF) at an urban and rural site of beijing atmos. Chem. Phys. 21, 14703–14724. https://doi.org/10.5194/acp-21-14703-2021.

Stein, A.F., Draxler, R.R., Rolph, G.D., Stunder, B.J.B., Cohen, M.D., Ngan, F., 2015. NOAA's HYSPLIT atmospheric transport and dispersion modeling system. Bull. Am. Meteorol. Soc. 96, 2059–2077. https://doi.org/10.1175/BAMS-D-14-00110.1.

Sutton, M.A., Dragosits, U., Tang, Y.S., Fowler, D., 2000. Ammonia emissions from non-agricultural sources in the UK. Atmos. Environ. 34, 855–869. https://doi.org/10.1016/S1352-2310(99)00362-3.

Tao, T., Shen, Z., Zhu, C., Yue, J., Cao, J., Liu, S., Zhu, L., Zhang, R., 2012. Seasonal variations and chemical characteristics of sub-micrometer particles (PM1) in Guangzhou, China, 2012 Atmos. Res. 118, 222–231. https://doi.org/10.1016/j.atmosres.2012.06.025.

Timonen, H., Mylläri, F., Simonen, P., Aurela, M., Maasikmets, M., Bloss, M., Kupri, H.-L., Vainumäe, K., Lepistö, T., Salo, L., Niemelä, V., Seppälä, S., Jalava, P.I., Teinemaa, E., Saarikoski, S., Rönkkö, T., 2021. Household solid waste combustion with wood increases particulate trace metal and lung deposited surface area emissions. J. Environ. Manag. 293, 112793 https://doi.org/10.1016/j.jenvman.2021.112793.

Trinh, T.T., Trinh, T.T., Le, T.T., Nguyen, T.D.H., Tu, B.M., 2019. Temperature inversion and air pollution relationship, its effects on human health in Hanoi City, Vietnam. Environ. Geochem. Health 41, 929–937. https://doi.org/10.1007/s10653-018-0190-0.

Turpin, B.J., Lim, H.-J., 2001. Species contributions to PM2.5 mass concentrations: revisiting common assumptions for estimating organic mass. Aerosol Sci. Technol. 35, 602–610. https://doi.org/10.1080/02786820119445.

U.S. EPA, 2013. Reference method for the determination of fine particulate matter as PM 2.5 in the atmosphere. 40 CRF 50.18. Appendix L. https://www.ecfr.gov/current/title-40/chapter-I/subchapter-C/part-50/appendix-Appendix%20L%20to%20Part%2050. (Accessed 9 February 2022).

US EPA, 2022. US EPA SPECIATE 5.2 repository. https://www.epa.gov/air-emissions-modeling/speciate.

Vestenius, M., Leppänen, S., Kyllönen, K., Hatakka, J., Hellén, H., Hyvärinen, A.-P., Hakola, H., 2011. Background concentrations and source apportionment of polycyclic aromatic hydrocarbons in south-eastern Finland. Atmos. Environ. 45 (20), 3391–3399. https://doi.org/10.1016/j.atmosenv.2011.03.050.

Vestenius, M., Hopke, P.K., Lehtipalo, K., Petäjä, T., Hakola, H., Hellén, H., 2021. Assessing volatile organic compound sources in a boreal forest using positive matrix factorization (PMF). Atmos. Environ. 259, 118503 https://doi.org/10.1016/j.atmosenv.2021.118503.

QCVN 05, Vietnam Environment Administration, Department of Science & Technology, 2013. National technical regulation on ambient air quality. https://123doc.net/document/3552983-qcvn-05-2013btnmt-national-technical-regulation-on-ambient-air-quality.htm.

Vuong, Q.T., Choi, S.-D., Bac, V.T., Thang, H.M., Hue, N.T., Lan, T.T., Hanh, D.T., Tuyen, T.V., Thang, P.Q., 2021. Spatial and temporal variations of the PM2.5 concentrations in Hanoi metropolitan area, Vietnam, during the COVID-19 lockdown. Int. J. Environ. Anal. Chem. 1–13. https://doi.org/10.1080/03067319.2021.1941918.

Watson, J.G., Chow, J.C., 2001. PM2.5 chemical source profiles for vehicular exhaust, vegetation burning, geological materials and coal burning in Northwestern Colorado during 1995. Chemosphere 43, 1141–1151. https://doi.org/10.1016/s0045-6535(00)00171-5.

WB, 2002. World Bank: an Overnight Success: Vietnam's Switch to Unleaded Gasoline. World Bank, Washington, DC (last access: 6 October 2021. https://openknowledge.worldbank.org/handle/10986/19894.

WHO, 2000. World health organization. In: Air Quality CGuidelines for Europe, second ed. WHO Regional Publications, European Series, Copenhagen, p. 91. 0378-2255.

WHO, 2021a. World Health Organization. WHO Global Air Quality Guidelines: Particulate Matter (PM2.5 and PM10), Ozone, Nitrogen Dioxide, Sulfur Dioxide and Carbon Monoxide. World Health Organization, Geneva, ISBN 978-92-4-003422-8 (electronic version), ISBN 978-92-4-003421-1 print version),).

WHO, 2021b. World Health Organization. More than 60 000 Deaths in Viet Nam Each Year Linked to Air Pollution last access: 15 September 2021. https://www.who.int/vietnam/news/detail/02-05-2018-more-than-60-000-deaths-in-viet-nam-each-year-linked-to-air-pollution.

Wu, J., Kong, S., Zeng, X., Cheng, Y., Yan, Q., Zheng, H., Yan, Y., Zheng, S., Liu, D., Zhang, X., Fu, P., Wang, S., Qi, S., 2021. First high-resolution emission inventory of levoglucosan for biomass burning and non-biomass burning sources in China. Environ. Sci. Technol. 55, 1497–1507. https://doi.org/10.1021/acs.est.0c06675.

Xing, Y.F., Xu, Y.H., Shi, M.H., Lian, Y.X., 2016. The impact of PM2.5 on the human respiratory system. J. Thorac. Dis. 8, E69–E74. https://doi.org/10.3978/j.issn.2072-1439.2016.01.19.

Xu, R.T., Pan, S.F., Chen, J., Chen, G.S., Yang, J., Dangal, S.R.S., Shepard, J.P., Tian, H. Q., 2018. Half-century ammonia emissions from agricultural systems in southern Asia: magnitude, spatiotemporal patterns, and implications for human health. GeoHealth 2, 40–53. https://doi.org/10.1002/2017GH000098.

Yan, Q., Kong, S., Yan, Y., Liu, X., Zheng, S., Qin, S., Wu, F., Niu, Z., Zheng, H., Cheng, Y., Zeng, X., Wu, J., Yao, L., Liu, D., Shen, G., Shen, Z., Qi, S., 2022. Emission and spatialized health risks for trace elements from domestic coal burning in China. Environ. Int. 158, 107001 https://doi.org/10.1016/j.envint.2021.107001.

Yang, X., Wang, T., Xia, M., Gao, X., Li, Q., Zhang, N., Yuan, G., Lee, S., Wang, X., Xue, L., Yang, L., Wang, W., 2018. Abundance and origin of fine particulate chloride in continental China. Sci. Total Environ. 624, 1041–1051. https://doi.org/10.1016/j.scitotenv.2017.12.205.

Yuan, Q., Qi, B., Hu, D., Wang, J., Zhang, J., Yang, H., Zhang, S., Liu, L., Xu, L., Li, W., 2021. Spatiotemporal variations and reduction of air pollutants during the COVID-19 pandemic in a megacity of Yangtze River Delta in China. Sci. Total Environ. 751, 141820 https://doi.org/10.1016/j.scitotenv.2020.141820.

Zhang, Y., Obrist, D., Zielinska, B., Gertler, A., 2013. Particulate emissions from different types of biomass burning. Atmos. Environ. 72, 27–35. https://doi.org/10.1016/j.atmosenv.2013.02.026.